

東海大學環境科學與工程學系

**Heterogeneous Catalytic Ozonation of Target
Pollutants using $\text{Fe}_3\text{O}_4/\text{SiO}_2/\text{Co}_3\text{O}_4$: Preparation and
Reaction Mechanism**

Lu, Li Wei

Advisor: Chang, Cheng Nan PhD

東海大學博士班研究生
論文指導教授推薦書

環境科學與工程學系 呂理維君所提之論文

題目：利用 $\text{Fe}_3\text{O}_4/\text{SiO}_2/\text{Co}_3\text{O}_4$ 催化劑催化臭氧降解水中目標污染物：材料製作與反應機制

Heterogeneous Catalytic Ozonation of Target Pollutants using $\text{Fe}_3\text{O}_4/\text{SiO}_2/\text{Co}_3\text{O}_4$: Preparation and Reaction Mechanism

係由本人指導撰述，同意提付審查。

指導教授： 張維南 (簽章)

107年4月20日

東海大學環境科學系博士班

論文口試委員審定書

環境科學與工程學系博士班呂理維君所提之論文

題目：利用 $\text{Fe}_3\text{O}_4/\text{SiO}_2/\text{Co}_3\text{O}_4$ 催化劑催化臭氧降解水中目標
污染物：材料製作與反應機制

Heterogeneous Catalytic Ozonation of Target Pollutants using
 $\text{Fe}_3\text{O}_4/\text{SiO}_2/\text{Co}_3\text{O}_4$: Preparation and Reaction Mechanism

經本委員會審議，認為符合博士資格標準。

論文口試委員召集人 李進浩 (簽章)

委員

張鎮南

彭嘉彬

陳谷叔

鄭文位

中華民國 107 年 4 月 20 日

致謝

感謝上帝，讓我撐過許多的困難，因靠著主得勝。感謝張鎮南 教授的指導，給予這麼好的研究環境以及給予寶貴經驗，在研究經費上從不間斷的幫助學生不半途而廢的走完博士班生涯，感謝彭彥彬 教授在論文撰寫與期刊文章著作上給予無私的指導，在博士班後期拔刀相助讓學生能夠在 2018 年被接受兩篇具代表性的國際期刊的文章。也謝謝老師時常給予學生開導，幫助我尋找人生的方向。同時謝謝宋孟浩 老師、陳谷汎 老師以及鄭文伯 老師在百忙當中擔任學生的口試委員並給予寶貴的指正和建議。

研究所生活當中，很感謝一起努力的實驗室夥伴們，感謝慧燕學姊的勉勵以及幫助，勳鍊學長、瀚賢學長感謝他們給予經驗幫助，博士班同學硯勳常與他一同討論功課讓我從中學習許多管理的知識，也感謝學生的工作伙伴，煊根、世軒、伊婷、貴樺、祐祺、茹茹、志哲、哲豪以及好甄，博士班的旅程中有你們的陪伴真的很棒，感謝主給予學生這麼棒的工作團隊，也願主蒙恩於你們，使你們在未來的工作生活可以天天都精采，每天的學習和挑戰將成為未來你們的盾牌，我會好好珍惜在一起的美好回憶。

在唸博士班窮學生時期，感謝文華補習班姜維老師與中興補習班給予舞台讓我成為化學補教老師，感謝帶領我成為化學老師的蕭堯老

師，讓我學習到教書的技巧，以及受到蕭堯老師許多在經濟上的幫助，也時常打電話關心學生與為我禱告，誠心感謝您的厚愛與無私的幫助，願神紀念蕭堯老師的擺上，希望未來有機會可以報答老師的恩惠。

感謝我的家人，給予我這麼大的支柱，不管在精神上、生活上、經濟上，不惜的給學生，讓我可以專心的在研究上，沒有你們的支持，我想就無法完成我的學業了，謝謝大家。



Abstract

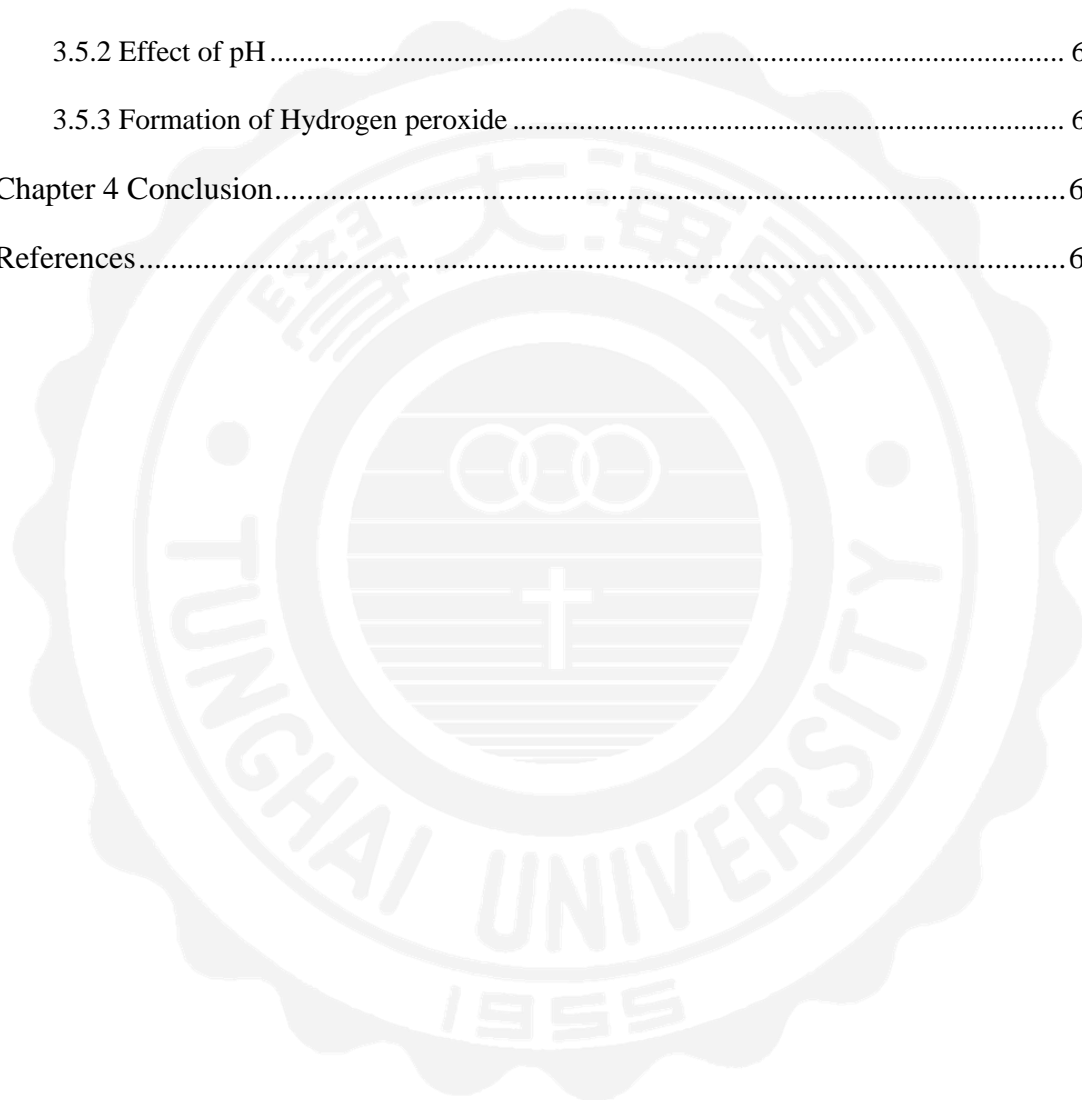
Heterogeneous catalytic ozonation is a novel type of AOPs to promote the capacity of oxidation. Co_3O_4 catalyst can catalyze ozone to generate free radicals and then achieve mineralization of dissolved organics effectively in water. Co_3O_4 could be supported on magnetic $\text{Fe}_3\text{O}_4/\text{SiO}_2$ for recovery. The presence of Co_3O_4 catalyst during ozonation at pH 5 as well as Mn-Pd catalyst at pH 11 results in the production of hydroxyl radicals, which acts as strong oxidants and react with organic pollutants. Catalyst which is covered by surface hydroxyl groups will be protonated or deprotonated when pH of solution is below or above pH_{pzc} . Catalytic ozonation of Methylene Blue and Diclofenac had the optimal condition of pH at 5 in accordance with pH of solution closed to pH_{pzc} , which can reach the activity of catalysts to generate more hydroxyl radicals. The surface hydroxyl groups of catalysts will be generated and revealed in solution to be $\bullet\text{OH}$ which is more powerful oxidant. Dosage of from 1.0 increased to 2.0 g/L, the TOC removal had not enhancement apparently. The enhanced generation of H_2O_2 in the catalytic ozonation has evidence for the development of DCF degradation. The TOC was insignificant decreased after 30 minutes in COP of pH5 and pH11. In SOP of pH5, the maximum yield of H_2O_2 that was generated 2.28 at 60 minutes and it was the lowest of all reaction.

Keywords: Heterogeneous Catalytic Ozonation, Co_3O_4 , diclofenac, methylene blue and H_2O_2

Content

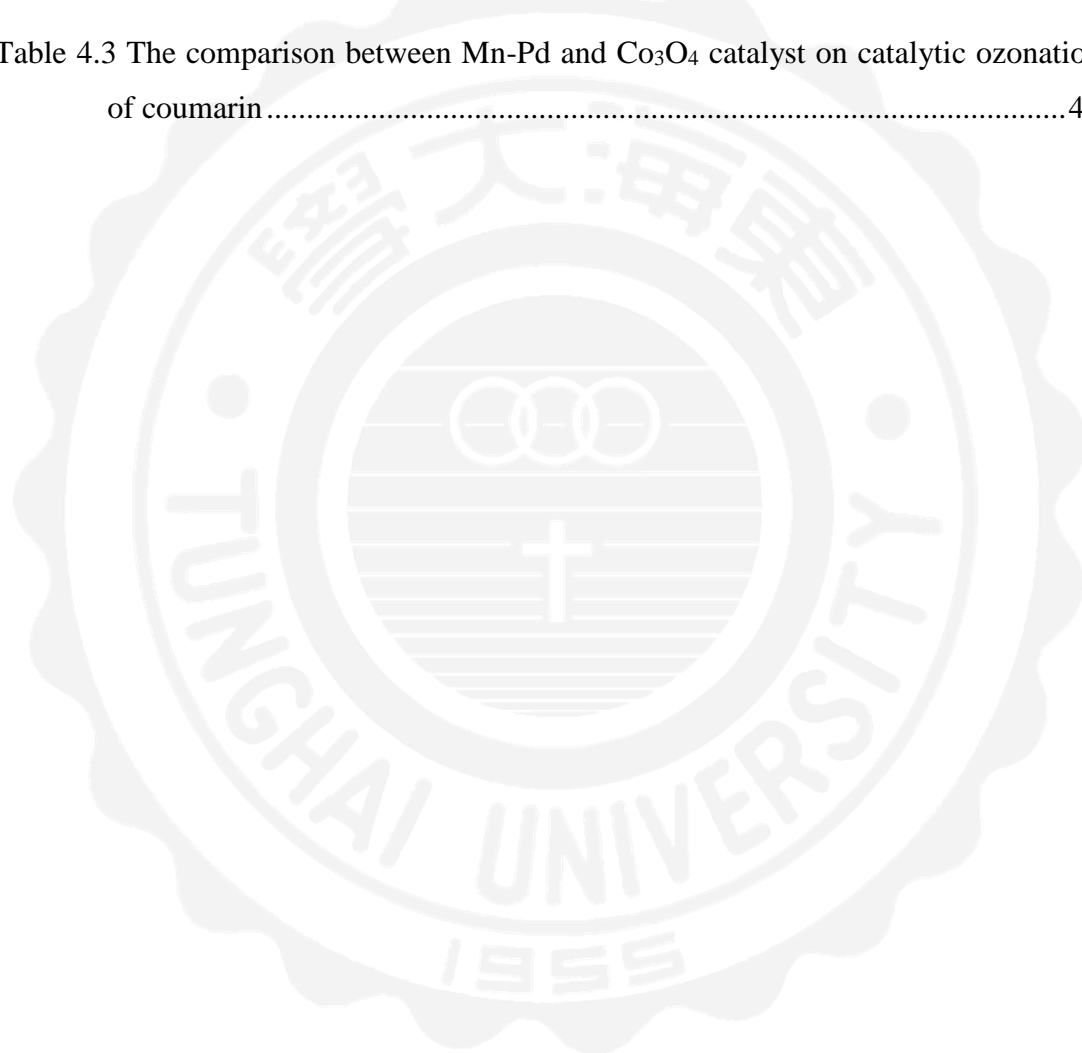
Chapter 1 Introduction	1
Chapter 2 Literature Review	5
2.1 Ozone.....	5
2.1.1 Direct reaction	6
2.1.2 Indirect reaction.....	8
2.2 Advanced Oxidation Processes (AOPs)	11
2.2.1 Catalytic ozonation.....	12
2.3 The effect of pH on heterogeneous catalytic ozonation	18
2.4 Target compounds	19
2.4.1 Humic acid and Trihalomethanes	19
2.4.2 Coumarin	21
2.4.3 Methylene Blue	22
2.5 Preparation of Catalyst.....	28
2.5.1 Precipitation.....	28
2.5.2 Impregnation.....	28
2.5.3 Bonding	29
Chapter 3 Materials and Methods	30
3.1 Preparation of catalyst	30
3.2 Analytical Method.....	31
3.2.1 Analysis of methylene blue and humic acid.....	31
3.2.2 Analysis of hydroxyl radical scavengers and diclofenac.....	31
3.2.3 Dissolved Organic Carbon	32
Chapter 4 Results and Discussion.....	35
4.1 Catalyst characterization	35
4.1.1 Comparison of the characteristic between $\text{Fe}_3\text{O}_4/\text{SiO}_2/\text{Co}_3\text{O}_4$ and $\text{Fe}_3\text{O}_4/\text{SiO}_2/\text{Mn-Pd}$	44

4.2 Comparison of decomposition of coumarin between $O_3/Fe_3O_4/SiO_2/Co_3O_4$ and $O_3/Fe_3O_4/SiO_2/Mn-Pd$	44
4.3 Reduction of THMFPS by $O_3/Fe_3O_4/SiO_2/Co_3O_4$ and $O_3/Fe_3O_4/SiO_2/Mn-Pd$	51
4.4 Catalytic ozonation of Methylene Blue by $O_3/Fe_3O_4/SiO_2/Co_3O_4$	55
4.5 Decomposition of Diclofenac by $O_3/Fe_3O_4/SiO_2/Co_3O_4$	57
4.5.1 Dosage loading	57
3.5.2 Effect of pH.....	60
3.5.3 Formation of Hydrogen peroxide	62
Chapter 4 Conclusion.....	64
References.....	66



List of Table

Table 2.1 Relative oxidation potentials [1].....	5
Table 2.2 The characteristic of Methylene blue.....	22
Table 2.3 Degradation of DCF on AOPs	27
Table 4.1 Analysis of elements on Fe ₃ O ₄ /SiO ₂ /Co ₃ O ₄ , (a) preparation with urea and (b) urea-free.....	37
Table 4.2 EDS and SQUID of Fe ₃ O ₄ /SiO ₂ /Co ₃ O ₄ and Fe ₃ O ₄ /SiO ₂ /Mn-Pd [62].	44
Table 4.3 The comparison between Mn-Pd and Co ₃ O ₄ catalyst on catalytic ozonation of coumarin	49



List of Figure

Figure 1.1 Flow chart in this study.....	4
Figure 2.1 Ozone decomposed by multi steps and chain processes [2].....	6
Figure 2.2 Dipolar cyclo addition [1]	7
Figure 2.3 Disintegration of ozonide [1].....	7
Figure 2.4 Reaction between phenol and ozone [1].....	7
Figure 2.5 Reactions of ozone in aqueous phase [8].	10
Figure 2.6 Mechanisms of catalytic ozonation in the presence of metals on supports (AH - organic acid; P, R - adsorbed primary and final by-products; P', R' - primary and final by-products in solution respectively)[28].	17
Figure 2.7 The structure of humic acid [31].	19
Figure 2.8 The structure of coumarin	21
Figure 2.9 Formation of 7-hydroxycoumarin in the reaction of coumarin with hydroxyl radicals [29].	21
Figure 2.10 The structure of Methylene Blue.....	22
Figure 2.11 The structure of diclofenac	24
Figure 2.12 Proposed degradation routes of DCF in Fe-MCM-41/O ₃ [9].....	26
Figure 2.13 Illustration of ionic bond and covalence bond on Fe ₃ O ₄ /SiO ₂	29
Figure 3.1. Schematic diagrams of ozonation system.....	34
Figure 4.1 XRD Patterns of catalyst before reaction.	36
Figure 4.2. The SEM/EDS image of Fe ₃ O ₄ /SiO ₂ /Co ₃ O ₄ , (a) preparation with urea and (b) without urea.....	36
Figure 4.3. FTIR spectra of particles for preparation (a)with urea, (b) without urea and (c) with urea after calcined.	38
Figure 4.4 XPS spectrum of Fe ₃ O ₄ /SiO ₂ /Co ₃ O ₄ and cobalt oxides, (a) urea-free and (b) urea-added are survey spectrum, (c) urea-free and (d) urea-added are Co2p.	40
Figure 4.5 Analyses of field-dependent magnetization hysteresis for Fe ₃ O ₄ , Fe ₃ O ₄ /SiO ₂ and Fe ₃ O ₄ /SiO ₂ /Co ₃ O ₄	42

Figure 4.7 Effect of pH on coumarin removal by C/C ₀ , (a) O ₃ /Fe ₃ O ₄ /SiO ₂ /Co ₃ O ₄ and (b) O ₃ /Fe ₃ O ₄ /SiO ₂ /Mn-Pd (C ₀ =100 mg/L, O ₃ concentration = 1.6mg/L and catalyst dosage: 1.0g/L).	47
Figure 4.8 Effect of pH on the production of 7-hydroxycoumarin on (a) O ₃ /Fe ₃ O ₄ /SiO ₂ /Co ₃ O ₄ and (b) O ₃ /Fe ₃ O ₄ /SiO ₂ /Mn-Pd (C ₀ =100 mg/L, O ₃ concentration = 1.6mg/L and catalyst dosage: 1.0g/L).	48
Figure 4.9 Effect of k _d value of coumarin at various pH on O ₃ /Fe ₃ O ₄ /SiO ₂ /Co ₃ O ₄ and O ₃ /Fe ₃ O ₄ /SiO ₂ /Mn-Pd (Experimental conditions: O ₃ concentration = 1.6 mg/L, pH of Fe ₃ O ₄ /SiO ₂ /Co ₃ O ₄ and O ₃ /Fe ₃ O ₄ /SiO ₂ /Mn-Pd at 5 and 11, respectively).	50
Figure 4.10 The effect of (a) A ₂₅₄ of NOMs decomposition and (b) DOC removal rates on O ₃ /Fe ₃ O ₄ /SiO ₂ /Co ₃ O ₄ and O ₃ /Fe ₃ O ₄ /SiO ₂ /Mn-Pd (Experimental conditions: O ₃ concentration = 1.6 mg/L, pH of Fe ₃ O ₄ /SiO ₂ /Co ₃ O ₄ and O ₃ /Fe ₃ O ₄ /SiO ₂ /Mn-Pd at 5 and 11, respectively).	53
Figure 4.11 Comparison of THMFPS decompositions in O ₃ /Fe ₃ O ₄ /SiO ₂ /Co ₃ O ₄ and O ₃ /Fe ₃ O ₄ /SiO ₂ /Mn-Pd (Experimental conditions: O ₃ concentration = 1.6 mg/L, pH of Fe ₃ O ₄ /SiO ₂ /Co ₃ O ₄ and O ₃ /Fe ₃ O ₄ /SiO ₂ /Mn-Pd at 5 and 11, respectively).	54
Figure 4.12 Effect of initial pH on degradation of Methylene Blue by catalytic ozonation (a) at various pH and (b) k _d value (C ₀ =100 mg/L, O ₃ =1.6 mg/L, initial dosage=1 g/L).	56
Figure 4.13 TOC removal (a) and k _{obs} value (b) at different doses of catalyst dosages (0.5, 1.0, 1.5, 2.0 g/L), (conditions of experiments: initial solution of DCF:50 mg/L; initial pH: 5, O ₃ =1.6 mg/L).	59
Figure 4.14 Effect of initial pH on (a)TOC removal and (b) k _{obs} value (conditions of experiments: initial solution of DCF:50 mg/L; catalyst concentration 1 g/L, O ₃ =1.6 mg/L).	61
Figure 4.15 Generation of H ₂ O ₂ in SOP and COP (conditions: initial concentration of DCF solution: 50 mg/L; catalyst concentration: 1g/L).	63

Chapter 1 Introduction

In recent years, organic residual waters from industries like textile, pharmaceutical and plastics have become an important threat to human health and the environment. The coloring organic compounds such as methylene blue with aromatic rings, and halide would increase their toxicity and decrease their biodegradability. Pharmaceutical residues in surface and ground waters have been a major environmental concern. Many pharmaceutical residues are non-biodegradable and resistant against conventional wastewater treatment. Diclofenac (DCF) is typical representatives of analgesic non-steroidal anti-inflammatory pharmaceutical compounds (NSAIDs). When DCF is exposures to environmentally relevant levels in water, toxicity and negative effect on aquatic life would be increased. Humic acids (HAs) are refractory large molecules and ozone can destroy them from large molecule to small molecule, and the efficiency of mineralization in ozonation is ineffective.

Advanced Oxidation Process (AOP) emerging water treatments are capable of removing organic or inorganic pollutants during treating wastewater or drinking water. There are different kinds of AOPs, such as ozonation, photo-catalysis and wet oxidation etc. widely used in purification process. The AOPs systems can generate free radicals, which are non-selective and very powerful oxidants for destructing refractory and hazardous pollutants.

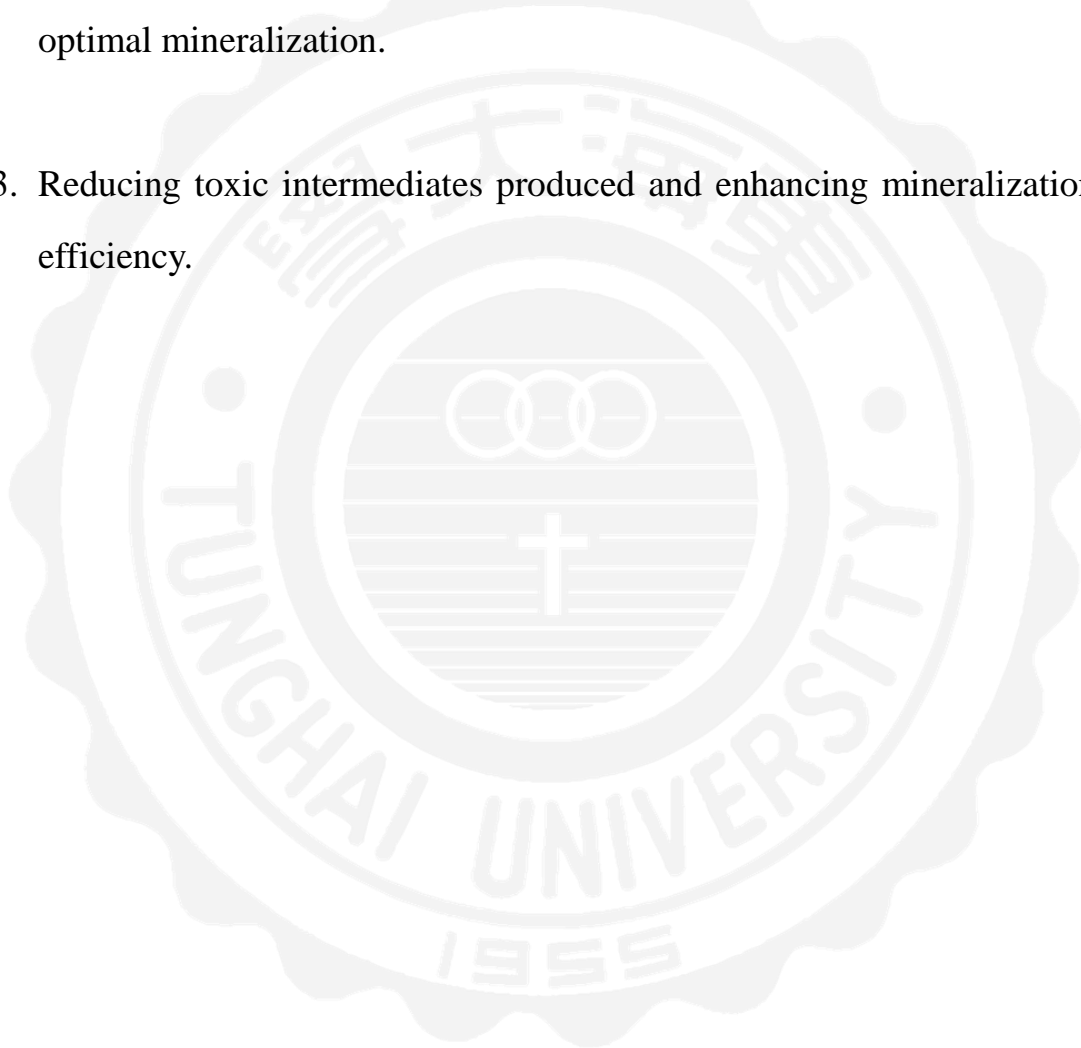
Ozone is capable of decomposing large amounts of organic substances, hence it is used to disinfect drinking water or treat wastewater in most countries. The advantage of ozonation is having high reaction rate, while

it also last little residual in water. However, ozone is with low solubility in water, therefore, it cannot prevent secondary pollutants in the distribution. Furthermore, the generation of ozone costs highly and attacks compounds selectively, and causes the limit of its application.

Catalytic ozonation is a way to generate more free radicals than ozone alone. Catalysts are able to decompose ozone effectively to transform free radicals as oxidants. The heterogeneous catalytic ozonation is a novel type of AOPs to promote the capacity of oxidation. The Cobalt oxide (Co_3O_4) catalyst can catalyze ozone to generate free radicals effectively and then achieve mineralization of dissolved organics easily in water. Cobalt oxide (Co_3O_4) could be supported on magnetic $\text{Fe}_3\text{O}_4/\text{SiO}_2$ for recovery. The investigation of the characteristics of the magnetic catalysts can be analyzed by the scanning electron microscopy with energy dispersive spectrometer (SEM/EDS), superconducting quantum interference device (SQUID), X-ray powder diffraction (XRD), Fourier-transform infrared spectroscopy (FTIR) and X-ray photoelectron spectroscopy (XPS).

Objectives

1. Investigate the effect of function group on surface particle during preparation
2. The mechanism of catalytic ozonation in target pollutants, diclofenac, Methylene blue and humic acid in different condition and pursue the optimal mineralization.
3. Reducing toxic intermediates produced and enhancing mineralization efficiency.



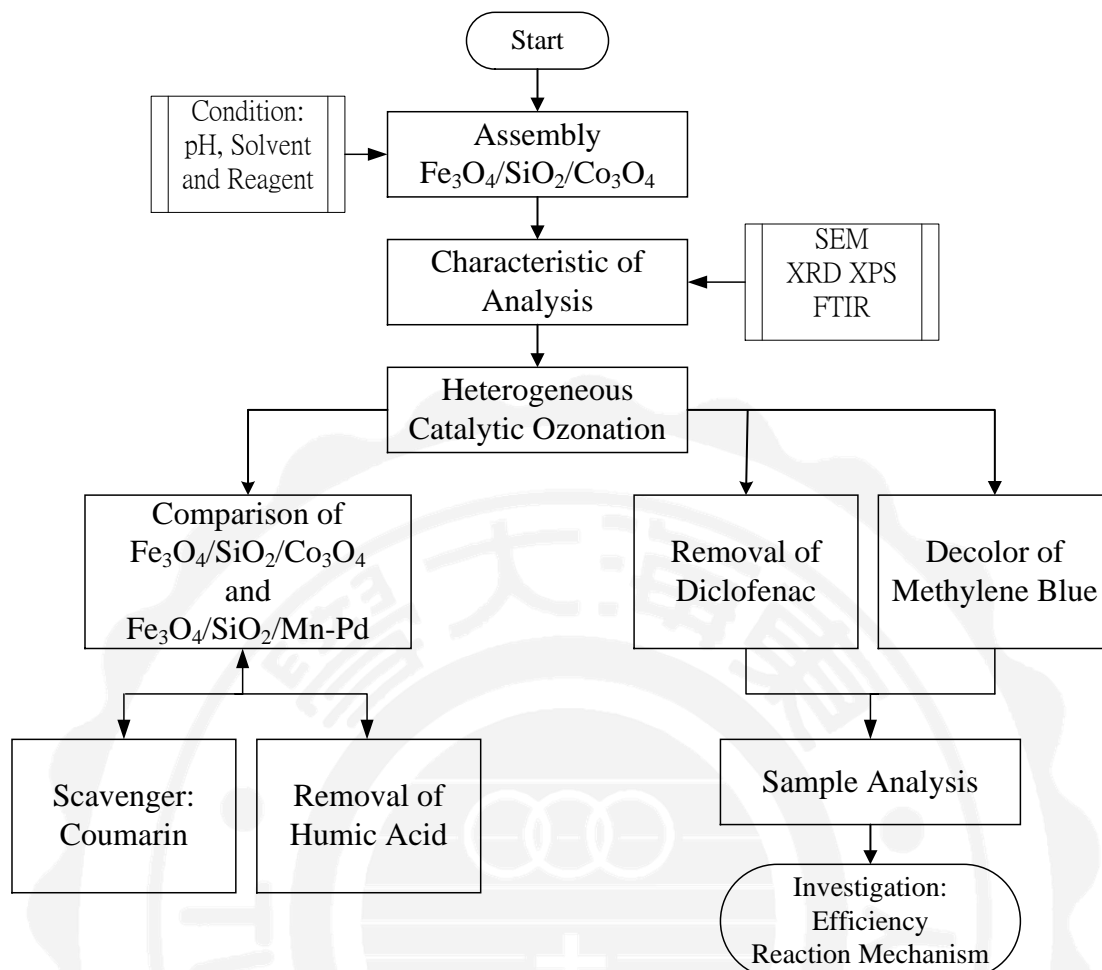


Figure 1.1 Flow chart in this study

Chapter 2 Literature Review

2.1 Ozone

Ozone is an allotrope of oxygen and a colorless gas. The melting and boiling point is -193°C and -112°C , respectively. The solubility of ozone in water is 1.09mg L^{-1} at 25°C , but it is able to solute in organic solution easily. The solubility of ozone in aqueous solution at 25°C is 13 times higher than oxygen. Ozone has a high oxidation potential ($\Delta G^{\circ}_f = 163.2$) and it also may decompose to free radicals which are more powerful oxidants to enhance oxidation process. The relative oxidation potentials are presented in Table 1.

Table 2.1 Relative oxidation potentials [1].

Species	Oxidation Potential, V
Fluorine	3.06
Hydroxyl radical	2.80
Nascent oxygen	2.42
Ozone	2.07
Hydrogen peroxide	1.77
Perhydroxyl radical	1.70
Hypochlorous acid	1.49
Chlorine	1.36

Hoigné-Staehelin-Bader and Gordon-Tomiyasu-Fukutomi [2] proposed that ozone decomposes in multiple steps and chain processes described by different mechanisms in aqueous solution, shown in figure 1.1.

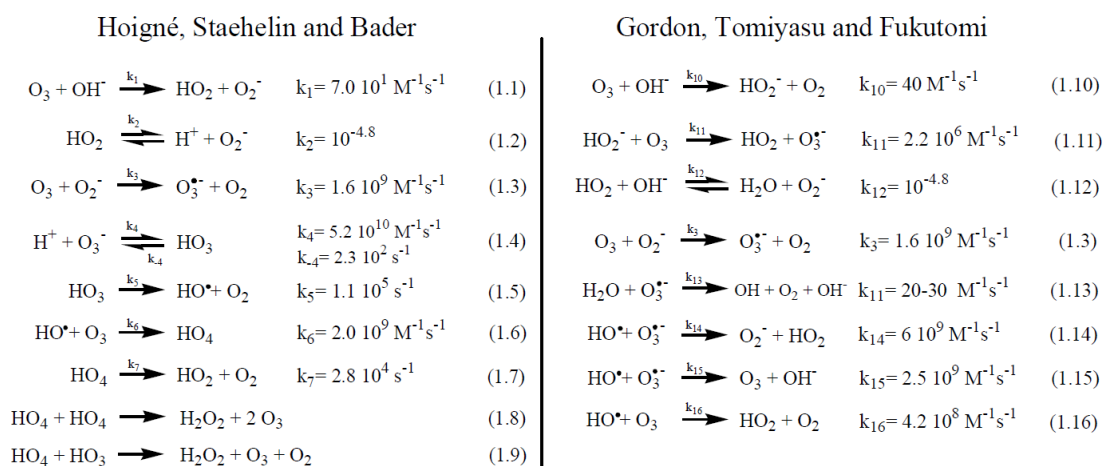


Figure 2.1 Ozone decomposed by multi steps and chain processes [2].

Ozonation has two ways to react with organic compounds in aqueous solution. Ozone can either react with compounds directly or decompose itself to generate $\bullet OH$ to react with organic compounds. Followings are the mechanisms for direct reaction and indirect reaction.

2.1.1 Direct reaction

The direct reaction of ozone with organic compounds is highly selective and causes slow rate reaction due to the chemical nature of ozone can act as dipole, nucleophilic agent and electrophilic agent which depends on the characteristic of reagents [2].

Cyclo addition (Criegee mechanism):

Ozone can undergo a 1-3 dipolar cyclo addition with unsaturated hydrocarbons to form a compound called ozonide. And then, ozonide disintegrates into an aldehyde, a ketone or zwitterion. Furthermore, Zwitterion can be broken down to hydrogen peroxide and carboxyl compounds shown in figure 1.2 and 1.3 [3].

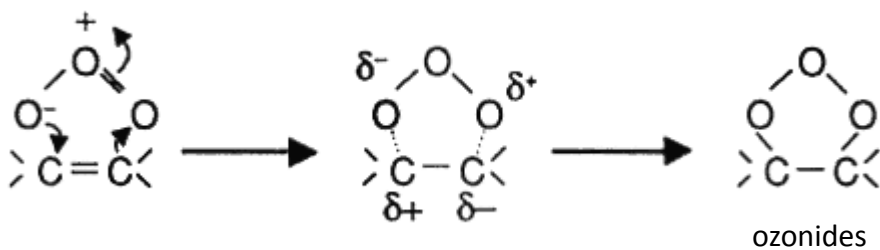


Figure 2.2 Dipolar cyclo addition [1]

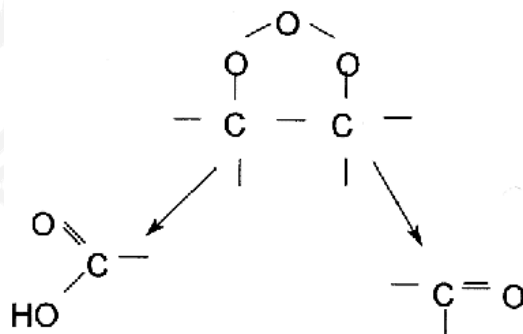


Figure 2.3 Disintegration of ozonide [1]

Electrophilic reaction

Ozone reacts actively with organic groups containing aromatic compounds with strong electronic density which are substituted by electron donor (such as $-\text{OH}$ and NH_2). Figure 1.4 is the example of a reaction between ozone and phenol. The reaction of ozone with aromatic compounds usually produces ozonides of benzenes and finally leading to the by-products would be produced such as aldehydes, ketones and organic acids [4].

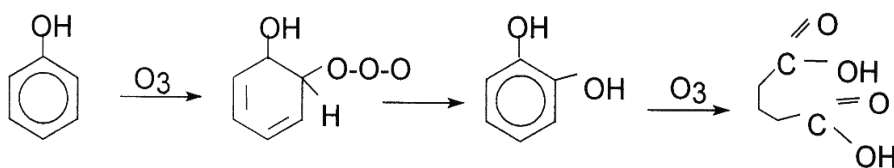


Figure 2.4 Reaction between phenol and ozone [1]

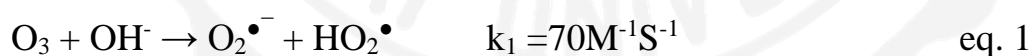
Nucleophilic reaction

Nucleophilic reactions mainly take place where there is a shortage of electrons and particularly at carbon compounds that contain electron withdrawing groups, such as $-\text{COOH}$ and $-\text{NO}_2$. The reaction is very limited and the rate is lower.

2.1.2 Indirect reaction

The indirect reaction involves the decomposition of ozone in water. Ozone reacts with hydroxide ions to generate $\bullet\text{OH}$ radicals which have much powerful oxidants and can quickly decompose organic compounds. This pathway is more complicated involved many factors for the mechanism. There are three main steps in mechanism of ozone decomposition that has explained by [5].

The first step is that ozone reacts with hydroxide ion (OH^-) to the formation of superoxide ions ($\text{O}_2^{\bullet-}$) and hydroperoxyl radicals (HO_2^\bullet). The reaction is more efficient in basic condition regards to the amount of OH^- which was shown in eq. 1 and 2.



which HO_2^\bullet can divide into superoxide ions and hydrogen ion:



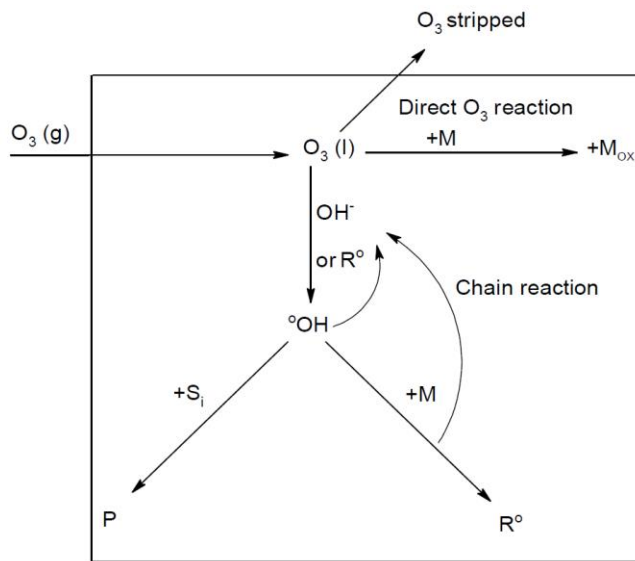
The second step is a chain reaction that O_3 reacts with $\text{O}_2^{\bullet-}$. The production of $\text{O}_3^{\bullet-}$ would react with hydrogen ion to become HO_3^\bullet which would be divided into hydroxyl radicals ($\bullet\text{OH}$).



The $\bullet\text{OH}$ would go further to react with ozone to form HO_4^{\bullet} , and then the HO_4^{\bullet} is divided into HO_2^{\bullet} and the reaction would go back to eq. 2 that was called chain reaction.

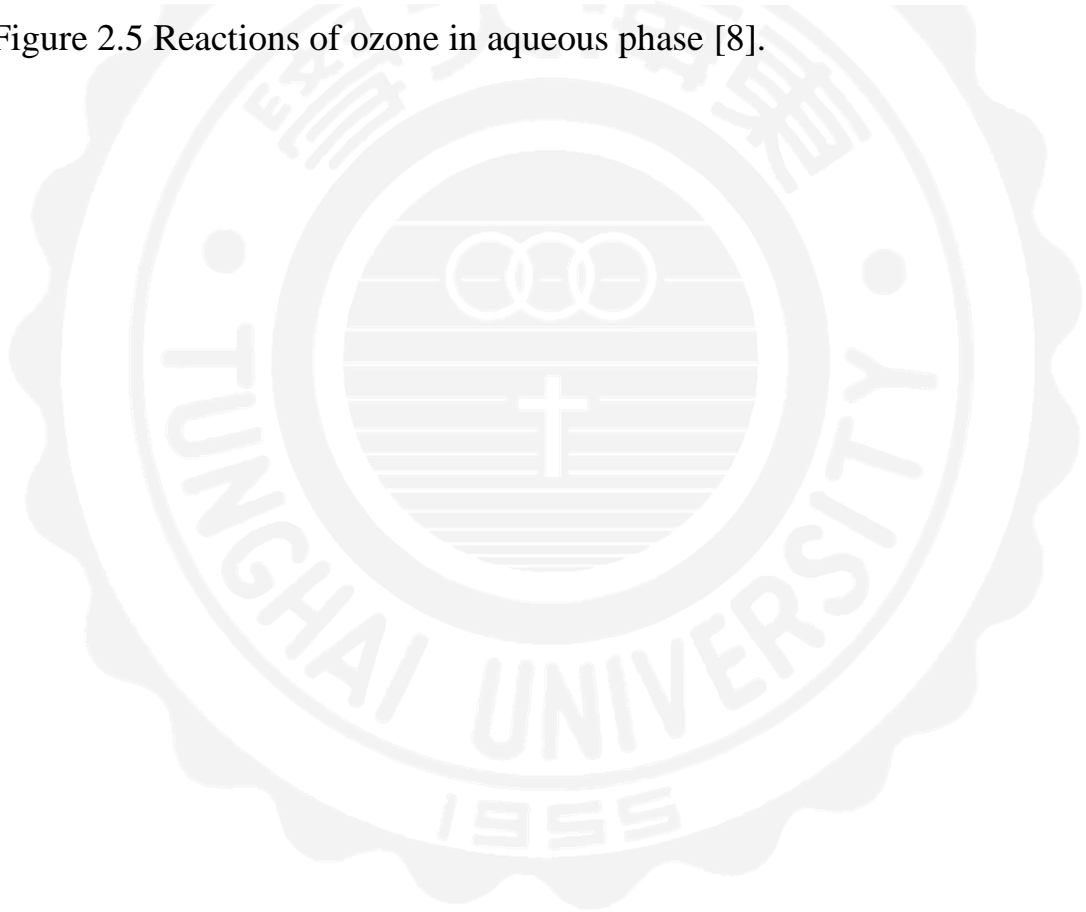
Ozone decreased in solution is significantly dependent on pH of solution involving the amount of hydroxide ion which is the initial decreasing step. The direct pathway is dominated under acidic condition ($\text{pH} < 4$) and indirect one is above pH 10 [6].

The demonstration of ozone oxidizes certain organic and inorganic compounds effectively. Ozone is high oxidant and application of water treatments which improved taste, color and disinfection. In order to higher oxidation potential than that of hydrogen peroxide, chlorine and hypochlorous, it has a great potential in water treatment. The ozonation of organic compounds occur a number of complicated reactions and many mechanisms have been presented in the literature [7]. In addition to direct oxidation, ozone decomposes via a chain indirect reaction mechanism depending on pH to form $\bullet\text{OH}$ radicals which is more powerful and non-selected oxidants [5]. However, the main disadvantages of ozonation are cost of generation and its highly selective oxidation power [8].



R= Free radicals, which catalyse the ozone decomposition
M= Solute
S_i= Hydroxyl radical scavenger
M_{ox}= Oxidized solute
P= Products, which do not catalyse the ozone decomposition

Figure 2.5 Reactions of ozone in aqueous phase [8].



2.2 Advanced Oxidation Processes (AOPs)

AOPs depend on to generate highly reactive hydroxyl radicals ($\bullet\text{OH}$). The AOPs offer a variety of feasible ways to generate hydroxyl radicals. The hydroxyl radicals are produced by former oxidants (ozone, hydrogen peroxide or oxygen) on special conditions (e.g. pH or temperature) that are catalyzed by energy sources (e.g. ultraviolet light or ultrasound) or catalysts (e.g. transit metal)[9]. The $\bullet\text{OH}$ are the strongest and non-selective oxidants that can be applied in water treatment and are able to oxidize the refractory compounds in aqueous solution. It enhances mineralization and reduces the incidence of byproducts produced. Some heavy metals can also be removed in forms of precipitated $\text{M}(\text{OH})_x$.

There have been various methods such as ultrasound, electrochemical, chemical and photochemical processes which used to produce $\bullet\text{OH}$. The processes above the statements may be classified into homogeneous and heterogeneous processes. In this study, we utilize heterogeneous catalytic process.

2.2.1 Catalytic ozonation

The development of efficient water treatment technologies, which remove organic pollutants such as solvents, dyes, pesticides, phenolic compounds or pharmaceuticals and personal care substances, has been attended [10]. Mineralization of refractory organic compounds is hardly to carry out by sole ozonation process (SOP) in many cases in which hydroxyl radicals cannot be generated due to the limited dissolved ozone [11]. To overcome the drawback, catalytic ozonation process (COP) can improve degradation efficiency emerged [12]. Catalytic ozonation allows a quicker removal of organic pollutants in accordance with catalysts improve the oxidizing power of ozone, markedly reducing the economic cost [13]. Catalytic ozonation has been applied to increase the efficiency for drinking water and wastewater treatment [12]. Catalytic ozonation includes homogeneous and heterogeneous method. Heterogeneous catalytic ozonation with an advantage over homogeneous catalytic system is the ease of catalytic retrieval from the reaction media [14].

Homogeneous catalytic ozonation

Due to improve ozonation efficiency and optimize economic efficiency, metal ion homogeneous ozonation of organic substrates is currently attracting considerable interest. Some research has been reported that some metal ions can decompose ozone leading to the generation of hydroxyl radicals [15]. Others have been suggested that metal ions can react with organic compounds to form complexes, which are subsequently oxidized [16]. Wu *et al.*, 2008 [17] reported that some metal ion/O₃ such

as Mn(II)/O₃, Fe(II)/O₃, Ni(II)/O₃ in references is more effective to decompose target pollutants than ozone alone, but some not at all because of suggesting that the catalytic performance in ozonation is quite compound-selective. In addition, the observed effects depend on such treatment conditions as pH and the ozone/catalyst ratio. The advantage of homogeneous catalytic ozonation is that effective surface sphere is not a problem and the mechanism is simple and easy to understand. However, some disadvantage which cannot be avoided is that the process involves the toxic or heavy metal in solution. The additional cost is required to remove metal ion and it cannot recover to reuse.

Heterogeneous catalytic ozonation

Heterogeneous catalytic ozonation is a technique which improves to generate more powerful oxidation for degrading or mineralizing organic pollutants in wastewater and drinking water treatments [18]. Especially solid catalyst has obtained an increasing interest in the drinking water or wastewater treatments because it is easy to separate from solution. Heterogeneous catalysts which are higher stability and lower loss can improve efficiency of treatment, and it are able to be recycled and reused without further treatment [19].

The preparation of metal oxide nanoparticles is a complex and still poorly understood process and many factors influence the precise form of prepared catalysts [20]. Co₃O₄ has been widely studied as heterogeneous catalysts for a while. However, the study on Co₃O₄ used as ozonation catalyst was rare [21]. In this study, Fe₃O₄/ SiO₂ would be the core/shell magnetic nanoparticles for recovery and then Co₃O₄ would be supported

on the core-shell particles to be main catalyst for ozonation.

Catalysts have two main mechanism of reaction. First, catalysts such as activated carbon adsorb the organic compounds to remove target pollutants, the others is that some elements such as transition metal are easy to switch electrons for redox. Legube and Karpel Vel Leitner (1999) [22] proposed the mechanism of catalytic ozonation that two assumptions can be described that:

Mecanism 1

1. Catalysts which is not catalytic effect but as adsorbents would adsorb organic acid (AH) by chemical adsorption ($AH + Me-OH \rightarrow Me-A$).
2. Ozone or $\bullet OH$ would oxidize the surface complex to give oxidation by-products either desorbed in solution (P' and R': primary and final by-products in solution, respectively) or still adsorbed at the surface of catalyst (P and R: adsorbed primary and final by-products, respectively).
3. The final adsorbed by-product (R) would desorb and thereafter be oxidized by ozone or $\bullet OH$.

Mechanism 2

1. Catalysts can be electron donator and react with ozone to be $\bullet OH$ in solution and then catalysts become oxidized status ($Me_{ox}-OH$).
2. AH would be adsorbed on oxidized catalysts that would be electron acceptor to oxidize AH then to be $Me_{red}A\bullet$.
3. The organic radical species $A\bullet$ would be then easily desorbed from catalyst and subsequently oxidized by OH or O_3 either in bulk solution, or more probably, into the thickness of electric double layer.

Qi *et al.*, 2015[23] had prepared copper ferrite as catalysts in catalytic ozonation of phenacetin. They proposed the pseudo first order kinetics of SOP eq.6 and catalytic ozonation process eq.7:

$$-\frac{d[PNT]}{dt} = k_1[O_3][PNT] + k_2 [\bullet OH][PNT] = k_{obs}[PNT] \quad \text{eq.6}$$

where $k_{obs} = k_1[O_3] + k_2 [\bullet OH]$

$$-\frac{d[PNT]}{dt} = k_1[O_3][PNT] + k_2 [\bullet OH][PNT] + k_3 [cata][PNT] = k_{obs-cata}[PNT]$$

where $k_{obs-cata}[PNT] = k_1[O_3] + k_2 [\bullet OH] + k_3 [cata]$ eq.7

k_3 is the adsorption rate constant of PNT by catalyst but it can be neglected due to PNT was not adsorbed on catalysts. It might be suitable to utilize these equations for this study.

Some references have been reported that using activated carbon [24] or nanotube [25] supported metal oxide as catalysts. Oxalic or oxamic acid which is not easy to be decomposed or mineralized by SOP can be adsorbed by activated carbon or nanotube. In this case, it is essential to consider which the main reaction is. Although the degradation of the target pollutant can be elevated, the mineralization would not be significantly enhanced. Some have been reported that metal oxide as catalysts in aqueous for catalyzing ozone to produce hydroxyl radical. It is more confident that the mineralization can be enhanced due to the hydroxyl radicals are gained in solution in particular condition.

This study points to new feasibilities for further research that cobalt oxide as catalyst for ozonation is still rare studies recently. Catalytic

ozonation of coumarin was observed the amount of hydroxyl radicals in different pH. The decomposition of methylene blue could be observed the efficiency of destain.

Co₃O₄ as catalyst

Co₃O₄ has been widely studied as heterogeneous catalysts, rechargeable batteries, solid-state sensors and catalyst for ozonation *etc* [21]. Catalytic mechanism of Co₃O₄ is very important for understanding the catalysis process. More important, many researchers had prepared Co₃O₄ as nanomaterials for enhancing the effectiveness. However, the recovery cannot be negligible. Many researches proposed that Co₃O₄ would be doped or supported on carriers which are able to be recovered, such as graphene [26] and red mud [27]. In this study, Co₃O₄ was supported on Fe₃O₄/SiO₂ core-shell particles which are capable of being magnetized.

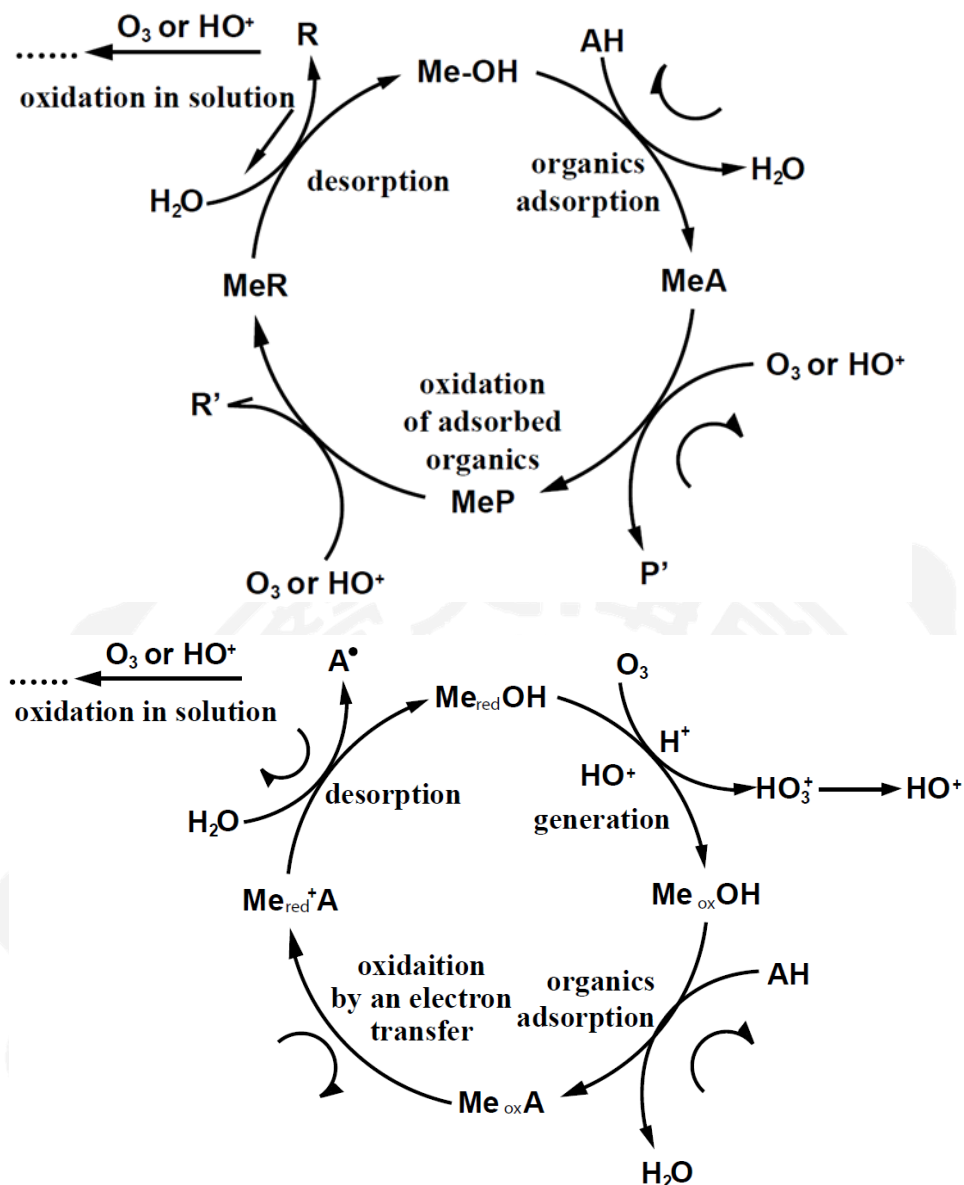
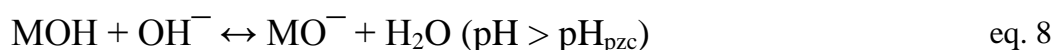
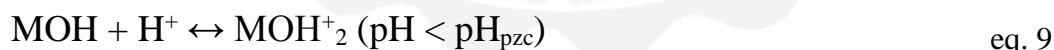


Figure 2.6 Mechanisms of catalytic ozonation in the presence of metals on supports (AH - organic acid; P, R - adsorbed primary and final by-products; P', R' - primary and final by-products in solution respectively)[28].

2.3 The effect of pH on heterogeneous catalytic ozonation

The pH of the solution exhibited a complicated effect on contaminants removal in COPs, since it affects ozone decomposition and the charge of surface catalysts. The example of Ikhlaiq *et al.*, 2012 [29] proposed the effect of pH in the presence of zeolites. It was stated that at $\text{pH} > \text{pH}_{\text{pzc}}$ zeolites are negatively charged and Lewis acid sites may be responsible for ozone decay. At $\text{pH} < \text{pH}_{\text{pzc}}$ the surface will be positively charged, and Bronsted acid sites on zeolite may be responsible for aqueous ozone decay and generation of hydroxyl radicals [30].

Huang *et al.*, 2015 [24] proposed that the catalytic activity of the catalyst reached its maximum as catalyst surface would be mostly zero charged ($\text{pH} = \text{pH}_{\text{pzc}}$). The protonation ($\text{pH} < \text{pH}_{\text{pzc}}$) process was strengthened with the decrease of solution pH, and then the interaction between surface hydroxyl groups and ozone was inhibited. The deprotonated ($\text{pH} > \text{pH}_{\text{pzc}}$) or neutral surface hydroxyl groups had a strong reactivity toward ozone [9]. However, the deprotonated form ($\text{pH} > \text{pH}_{\text{pzc}}$) can cause catalysts to be negative charged that would lead to reduced surface OH-ozone interaction chances. So the uncharged surface was more active than protonated or deprotonated form.



2.4 Target compounds

2.4.1 Humic acid and Trihalomethanes

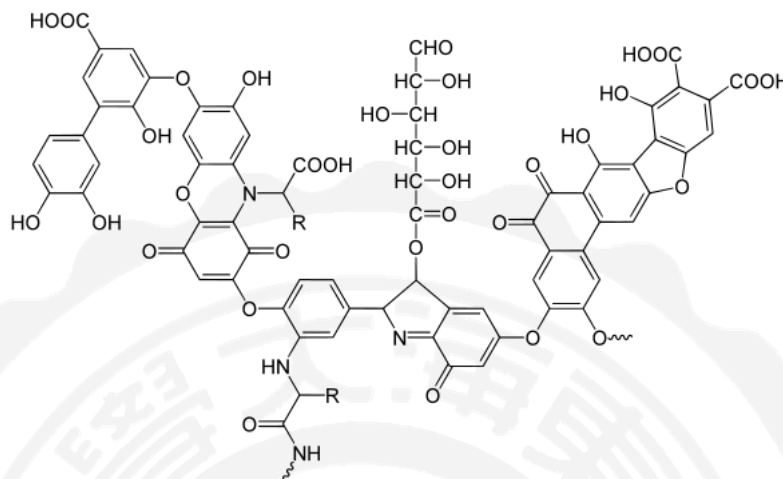


Figure 2.7 The structure of humic acid [31].

The natural organic matters (NOM) compose mainly of humic substances which serve as the major precursor to the formation of disinfections. One of the most significant problems in drinking water treatment is the formation of disinfection by-products (DBPs) [32]. Physical and chemical fractionation of aquatic NOM at specific pH can be used to classify organic solutes into broadly defined hydrophobic and hydrophilic fractions. Moreover, the hydrophobic fraction is thought to be the most important precursor for trihalogenmethane (THM) formation [33]. The different NOM fractions present different properties in term of chlorine and ozone reactivity and disinfection by-product formation potential (DBPFP). Carboxylic functional groups account for 60-90% of all functional groups and they are negatively charged at the pH range of natural waters THMs and haloacetic acids (HAAs) are the two most abundant groups of disinfection by-products found in chlorinated waters

[34]. Ozone has proven the ability to decrease the concentration of DBP precursors and a number of microorganisms, and reacts with organic substances to increase their biodegradability [34]. However, ozone is a selective reaction with NOM. AOP is the effective way to generate hydroxyl radicals which non-selective oxidants by ozone decomposition that is so-called “heterogeneous catalytic ozonation in this study.



2.4.2 Coumarin

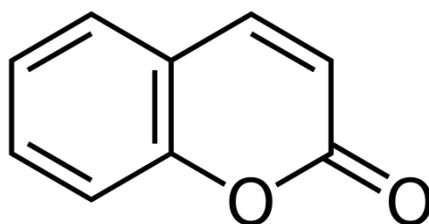


Figure 2.8 The structure of coumarin

Coumarin is used in the pharmaceutical industry as a precursor molecule in the synthesis of anticoagulant pharmaceuticals [35]. Coumarin has been used as a probe molecule as it is known to react with hydroxyl radicals leading to the formation of fluorescent 7-hydroxycoumarin [29]. 7-hydroxycoumarin which has been detected during the experiment can represent indirectly the amount of hydroxyl radicals and comparison of every experimental group in different conditions.

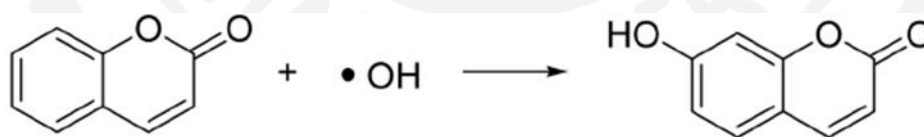


Figure 2.9 Formation of 7-hydroxycoumarin in the reaction of coumarin with hydroxyl radicals [29].

2.4.3 Methylene Blue

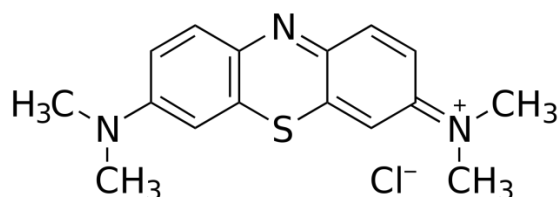


Figure 2.10 The structure of Methylene Blue.

Methylene blue is a heterocyclic aromatic chemical compound and it is a cationic and aromatic stain that is soluble in water and alcohol.

Table 2.2 The characteristic of Methylene blue

Characteristic	
Chemical formula	C ₁₆ H ₁₈ N ₃ SCl
Molar mass	319.85 g/mol
Melting Point	100°C to 110°C
Boiling Point	Decomposes
Solubility in water	43,600 mg/L at 25 °C
pKa	3.8

It deteriorates water quality by reducing the dissolved oxygen, which modifies the properties and characteristics of aqueous fluids and causes toxic effects on aquatic organisms, among other problems [36]. Methylene blue has been charged by various industries and has been influencing the water color and turbidity. Moreover, it threatens human and animal health, causing breathing difficulties, nausea, vomiting, sudoresis [37] and potential carcinogenicity of certain organic dyes [38]. Since dyes are intentionally designed to resist chemical and microbial attacks to keep the color stability. Conventional biological wastewater treatment methods are ineffective in removing the color. Adsorption has been developed to

effectively remove methylene blue in waste water. However, desorption might be a potential problem in physical methods.

In this study, $\text{Co}_3\text{O}_4/\text{SiO}_2/\text{Fe}_3\text{O}_4$ is used as catalyst for catalytic ozonation of methyl blue, anionic dye molecule from aqueous medium which is harmful to human being regarding to its mutagenic effect (Ferguson *et al.* 1988).



2.4.4 Diclofenac

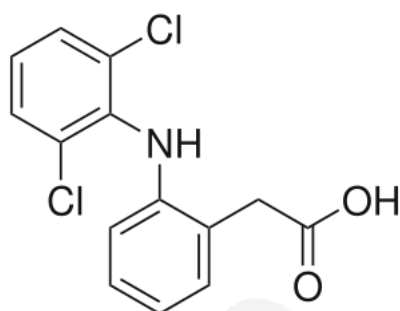


Figure 2.11 The structure of diclofenac

Among the large number of various organic pollutants into the water resources, pharmaceutical residues are not fully degraded in conventional wastewater treatment plants and are continuously released in the aquatic environment resulting in finding their way into surface, ground waters and even drinking water and can have devastating effects on the environment[39] and may cause risks to human health.

Diclofenac (DCF) is a nonsteroidal anti-inflammatory pharmaceutical compounds (NSAIDs) taken to reduce inflammation and as an analgesic reducing pain and have been recently detected in the aquatic environment [40]. The ecotoxicity of NSAIDs such as DCF alone is relatively low, but prolonged exposure to environmentally relevant concentrations up to $\mu\text{g/L}$ range and caused bioaccumulation to animals [41].

Biological treatments seem to be inefficient to remove this compound as literature being proposed [42]. Huang *et al.*, 2017[43] proposed that conventional wastewater treatment processes such as filtration or activated sludge could only remove 20–30%. Various advanced oxidation processes (AOPs) have reported in the literature for the degradation and removal of residual pharmaceuticals are successful and promising methods from aqueous solution[40]. Degradation of DCF was investigated in several

reports using photolysis and photocatalytic degradation[44], sonolysis[45], ozonation[42] and combined application[9]. Among these processes, a high DCF removal efficiency and high mineralization were obtained in a short reaction time. Degradation pathway and ecotoxicity of DCF remains to have to be investigated and conducted.

SOPs led to high DCF removals in a short reaction period according to the high rate constant of the direct reaction [46]. However, ozonation is not quite efficient mineralization [47]. COPs have much attention for its potential of removal DCF [9]. Catalysts such as metal, metal oxide or activated carbon in ozonation would enhance to generate more powerful active species against the toxic by-product produced. Among various solid catalysts, unsupported transition metal oxide such as MgO [48], TiO₂ [49] and MnO₂ [50] were frequently employed and found to be efficient for catalytic ozonation of pollutants. In order to increase its active sites, metal or metal oxides were often coated or doped on supporters [9] such as Al₂O₃ [51], activated carbon [52] and SiO₂ [53].

The accumulation of organics on the surface of catalyst could improve the utilization efficiency of active species derived from ozone decomposition. However evidences also showed that the adsorption of organics may lower the catalytic performance.

Some studies proposed the degradation pathway of DCF with oxidant species. Chen *et al.*[9] revealed the 2 pathways for degradation of DCF. The NH-bridge between the aromatic rings was also cleaved by O₃ and/or •OH first in path 1, and then the electron-withdrawing effect of –Cl and –CH₂COOH, •OH was more likely to substitute meta of –Cl and –CH₂COOH group on aromatic ring. In Path 2, DCF was reacted with •OH

and generated D4 (in figure 1.12). Then the $\bullet\text{OH}$ would further oxidize the intermediates to lead to the dehalogenation and the opening ring of aromatics. The powerful oxidants, $\bullet\text{OH}$, can decompose DCF effectively accordance with the references following the table 1.3.

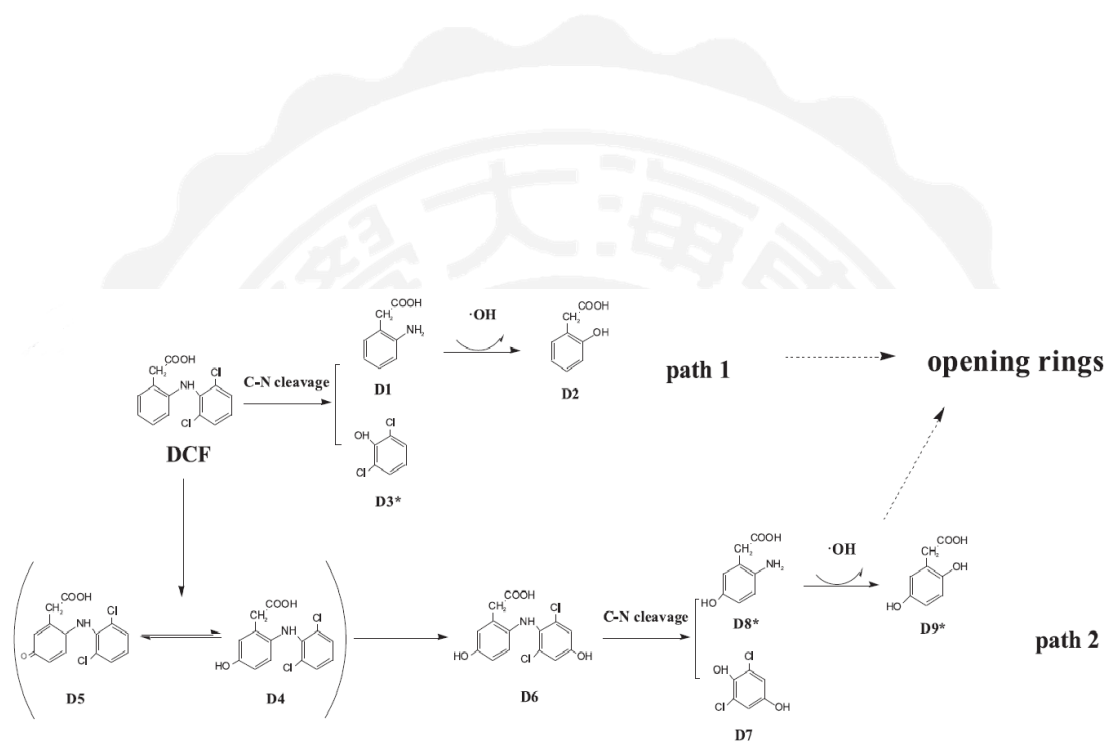


Figure 2.12 Proposed degradation routes of DCF in Fe-MCM-41/O₃ [9]

Table 2.3 Degradation of DCF on AOPs

	Title	Conditions	Ref.
Catalytic Ozonation			
Beltran <i>et al.</i> , 2009	Diclofenac removal from water with ozone and activated carbon	$C_0=30\text{mg L}^{-1}$ pH 7	[52]
Gao <i>et al.</i> , 2017	Mechanism of enhanced diclofenac mineralization by catalytic ozonation over iron silicate-loaded pumice	O_3 dose: 5.52 mg L^{-1} Catalyst dose: 800mg L^{-1} $C_0=29.6\text{ mg L}^{-1}$ pH 7	[54]
Chen <i>et al.</i> , 2016	Effective mineralization of Diclofenac by catalytic ozonation using Fe-MCM-41 catalyst	O_3 dose: 100 mg h^{-1} Catalyst dose: 1g L^{-1} $C_0=20\text{ mg L}^{-1}$ pH 7	[9]
Photocatalysis			
Cheng <i>et al.</i> , 2016	A facile and novel strategy to synthesize reduced TiO_2 nanotubes photoelectrode for photoelectrocatalytic degradation of diclofenac	Lamp: 35W $C_0=5\text{ mg L}^{-1}$	[55]

2.5 Preparation of Catalyst

2.5.1 Precipitation

Co-precipitation is a method to assemble materials for metal oxidants adding precipitation agent. Applying co-precipitation can control particle size and provide several possibilities to modify the particle surface and shape due to dependent on the pH of concentration of the initial materials. However, it is not easy that metal was coated on other metals evenly. Precipitation of various cobalt salts from aqueous or alcoholic-aqueous solutions yields cobalt oxide nanoparticles.

2.5.2 Impregnation

It is a commonly technique used for the synthesis of heterogeneous catalysts. The active metal precursor is dissolved in an aqueous or organic solution. Then the metal-containing solution is added to a catalyst support containing the same pore volume as the volume of the solution. Impregnation can be termed wet or dry, depending whether the volume of the impregnating solution is greater than or equal to the pore volume of the support (Bourikas *et al.*, 2007).

2.5.3 Bonding

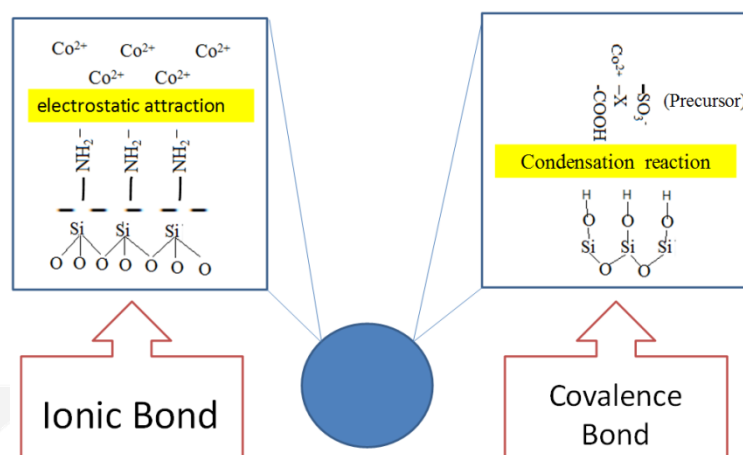


Figure 2.13 Illustration of ionic bond and covalence bond on $\text{Fe}_3\text{O}_4/\text{SiO}_2$.

Metal oxides or compounds have two synthetic methods generally to be bonded on silicate, ionic bond and covalence bond. Bao et al., 2016 [56] had been proposed that (3-aminopropyl)-triethoxysilane (a common silanizing reagent) were used as surface modification reagents, and modify $\text{Fe}_3\text{O}_4@\text{SiO}_2$ to get a novel amino-functionalized $\text{Fe}_3\text{O}_4@\text{SiO}_2$ nano-sorbents ($\text{Fe}_3\text{O}_4@\text{SiO}_2\text{-NH}_2$) for capturing metal ion effectively. Functionalized method has an efficient way that metal doped on SiO_2 .

Ionic Bond:

Coulomb electrostatic force would make cobalt ion to combine with the surface of particle which has to be bonded by nucleophile-ligand.

Covalence Bond:

The precursor of metal compounds such as acetyl, sulfur and halide can bond with silicate of surface and is prepared by wetness impregnation in organic solution.

Chapter 3 Materials and Methods

3.1 Preparation of catalyst

1. Preparation of core (Fe_3O_4)

Preparation of Fe_3O_4 is the mixture of $\text{FeCl}_2 \cdot 4\text{H}_2\text{O}$ (2.536g) and FeCl_3 (9.740g) in ammonia solution in specific ratio at 75°C . Then, magnet is used to separate solid from liquid.

2. Preparation of core/Shell ($\text{Fe}_3\text{O}_4/\text{SiO}_2$)

Tetraethyl orthosilicate (TEOS) (15mL) is precursor of SiO_2 which would be coated on Fe_3O_4 . The solution with water, ammonia and isopropanol mixed added to Fe_3O_4 and shook 30 minutes. The solution is stirred for 500 rpm when added TEOS very slowly at 40°C for 5 hours.

3. Preparation of Co_3O_4 coated on $\text{Fe}_3\text{O}_4/\text{SiO}_2$

$\text{Co}(\text{OH})_3 \cdot (\text{H}_2\text{O})_6$ (20.4g) as precursor is added to the solution and form $\text{Fe}_3\text{O}_4/\text{SiO}_2$ in ethanol solution. The solution is shaken for 24 h then dried for 24 h and calcined at 600°C .

The precursor of cobalt compounds combine with $\text{Fe}_3\text{O}_4/\text{SiO}_2$ and chemical A by wetness impregnation in ethanol solution ($>95\%$ v/v). The solution is shaken for 24 hours and then calcined at 350°C

3.2 Analytical Method

3.2.1 Analysis of methylene blue and humic acid

The A_{664} is measured for methylene blue with a spectrophotometer (U-2800A, Hitachi Co., Japan). Set the deionized water into 1 cm quartz cell as blank and then adjust the absorbance to zero. Take the water sample into the cell hold, and the data is recorded. Humic acid concentration was analyzed by UV absorbance at a wavelength of 254 nm with a spectrophotometer (U-2800A, Hitachi Co., Japan).

3.2.2 Analysis of hydroxyl radical scavengers and diclofenac

Hydroxyl Radical scavengers

The HPLC system with reverse phase column for the chromatographic analysis is consisted of a PU-980 type pump (Jasco CO., Japan) and an UV-975 type detector and. The column is a Pharmacia C₂-C₁₈ μ RPC column ST 4.6/100 (5 μ m, 4 mm ID x 15 cm) with volume of 1.66mL. For all HPLC analysis, the elution solution consisted of methanol and deionized water (V/V=70:30) was used with flow rate of 0.5 mL/min. The absorbance of coumarin and 7-hydroxycoumarin were measured at wavelength 320 nm, which was chosen due to obtain the maximum sensitive detection.

Analysis of DCF

The concentration of Diclofenac was analyzed by a high performance liquid chromatography (HPLC, LC10A, Shimadzu, Japan) with a UV

detector (SPD-10AV) at 277 nm using the following conditions: column, Diamon-sil 5U C18.

3.2.3 Dissolved Organic Carbon

The analysis procedure of DOC is according to the Standard Methods 21st Ed., 5310D (APHA *et al.*, 2005). The concentrations of DOC were determined by a TOC analyzer (Model 1010, OI., USA). The wet-oxidation method is utilized to analyze the dissolved organic matter in the water sample. The organic matter which can pass through the 0.45 μ m membrane as the DOC defined. After the oxidant (sodium persulfate, Na₂S₂O₈) was added to the digester, the mixture temperature is raised to 100 °C. Then, the CO₂, which was formed the organic carbons is passed through a dried oven for analytic form NDIR (nondispersive infrared spectrometry) to quarantine analytic of the DOC concentration. The Milli-Q water was used for all dilutions, sample preparation, and final glassware cleansing in this work. The calibration curves were constructed by preparing standards at 0, 0.5, 1, 2, 2.5 and 5 mg/l.

Table 3.2 Summary of the reagent and equipment for DOC test.

Reagent	Series Number, Maker, Country
Na ₂ S ₂ O ₈	1.06609.0500, Merck, Germany
H ₃ PO ₄	1.00573.1000, Merck, Germany
KHP*	1.02400.0080, Merck, Germany
Equipment	Series Number, Maker, Country
TOC	Model 1010 O.I. Analytical, USA

*Stock solution: 2.128 g KHP in 1 L reagent water (1,000 mg-C/L)

3.2.4 Analysis of Trihalomethanes (THMs)

The THMs analysis was according to the Standard Methods 21th ed., 6232D [57]. A 5 mL sample was pretreated by using a purge & trap instrument (Eclipse model 4660, O.I. Analytical, USA) and then automatically injected into a gas chromatography equipped with an electron capture detector (GC/ECD) (GC-14B, Shimadzu Co., Kyoto, Japan) connected to a recorder (SIC Chromatocorder 12, Alphatech Corp., Tokyo, Japan).

Instruments

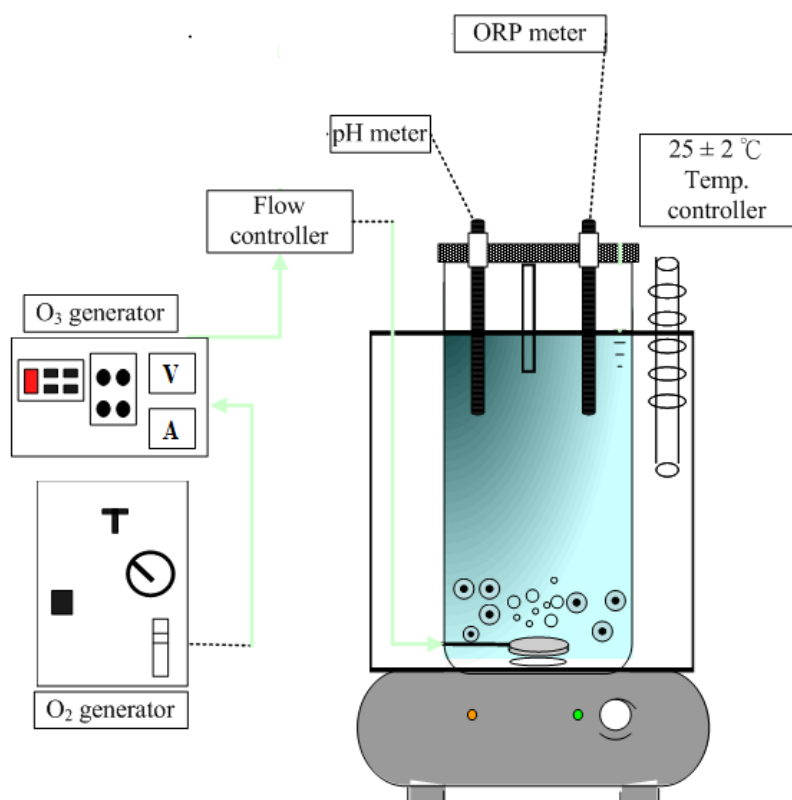


Figure 3.1. Schematic diagrams of ozonation system.

Figure 3.1 shows the 3-Liter batch Pyrex glass reactor equipped with a 500 rpm mixer and three monitored sensor (pH, ORP and DO₃). The temperature of reaction was maintained at $25 \pm 2^\circ\text{C}$ by water bath. Ozone molecules generated with ozone generator (AirSep. Corp., KA-1600, USA). The flow rate of ozone stream was controlled by a mass-flow controller and continuously introducing into the reactor at a flow rate of $4,000 \pm 23$ mL/min.

Chapter 4 Results and Discussion

4.1 Catalyst characterization

Figure 4.1 showed that X-ray diffraction of the catalyst consisted of Fe_3O_4 , SiO_2 and CoO_x , and therefore it could be characterized as $\text{Fe}_3\text{O}_4\text{-SiO}_2/\text{CoO}_x$. According to the XRD patterns of the Co_3O_4 [58]. The CoO_x on the $\text{Fe}_3\text{O}_4/\text{SiO}_2$ is existed in Co_3O_4 . The peaks at $2\theta=31.3^\circ$, 36.9° , 44.8° , 59.4° , and 62.9° ($d=1.43$) correspond to the (220), (311), (400), (511) and (440) planes of the Co_3O_4 cubic structure, respectively (Chen *et al.*, 2008). However, some peaks corresponding to Fe_3O_4 and Co_3O_4 were difficult to distinguish in XRD.

Due to the solvent was ethanol in acidic condition, the cobalt was inefficient to be coated on SiO_2 . On the contrary, the cobalt was coated on SiO_2 efficiently in basic condition of solution. The figure 4.2 showed the SEM/EDS image of catalyst. EDS analysis was used to investigate the chemical composition of the catalyst, which indicated that the $\text{Fe}_3\text{O}_4/\text{SiO}_2/\text{Co}_3\text{O}_4$ are composed of Fe, O, Si and Co and weight % is 31.75, 17.28%, 21.16% and 16.00% for preparation without urea and 33.82, 24.05%, 14.41% and 27.72% for preparation with urea, respectively (shown in Table 3.1). Figure 4.3 (a) showed the SEM/EDS image of catalyst prepared by urea and the weight% is 27.72%, the cover rate is promoted to 13% compared to urea-free group.

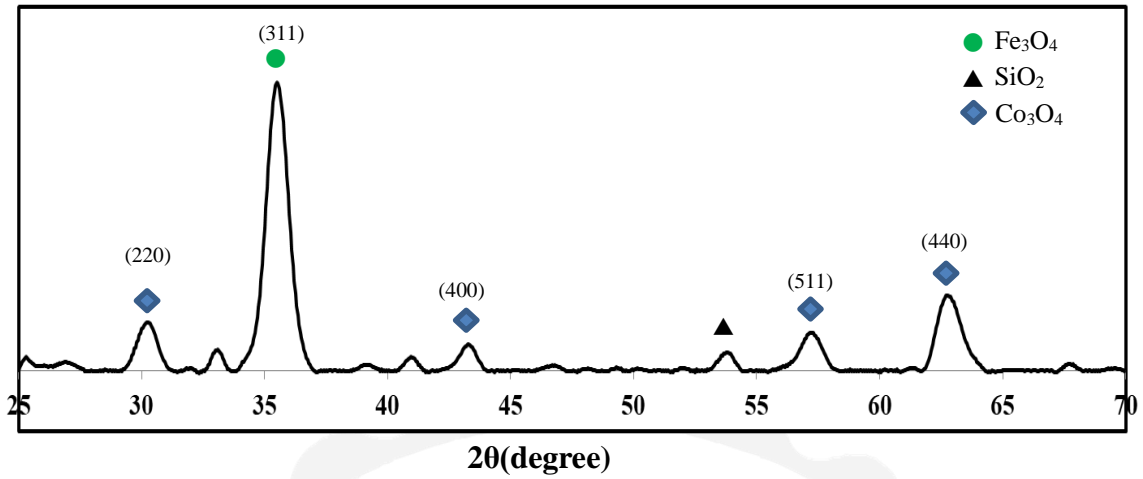


Figure 4.1 XRD Patterns of catalyst before reaction.

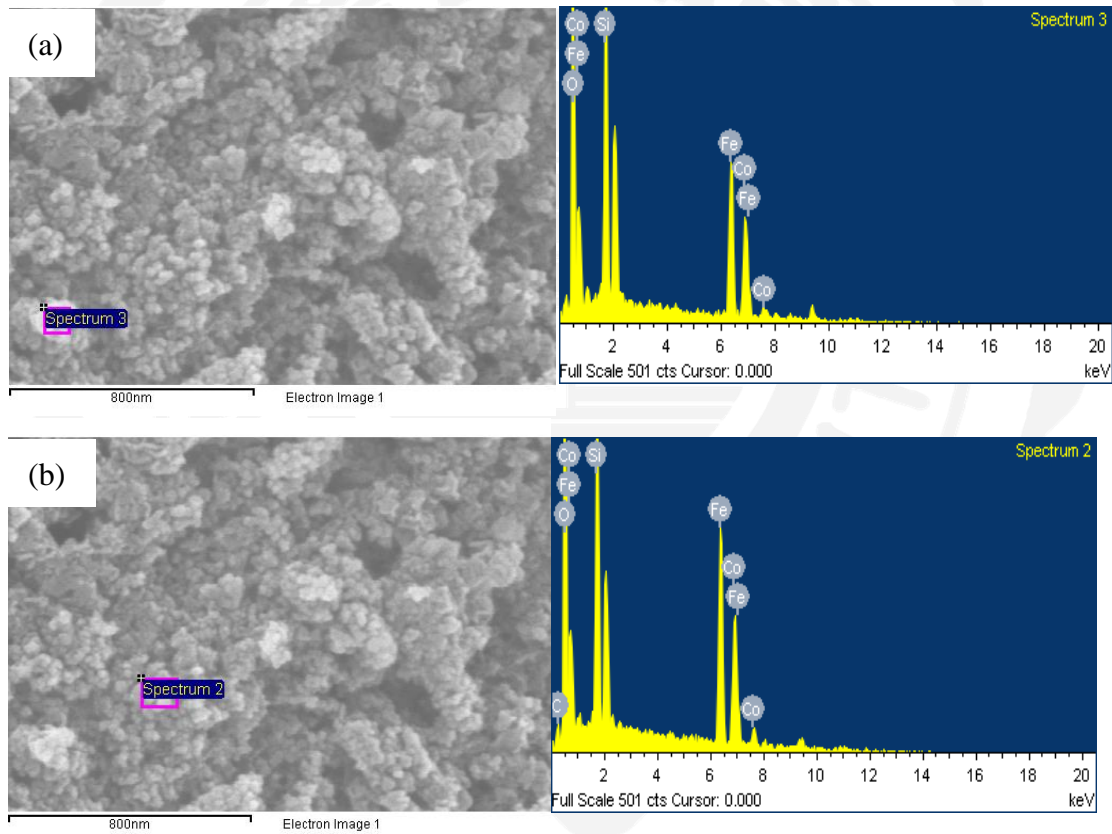
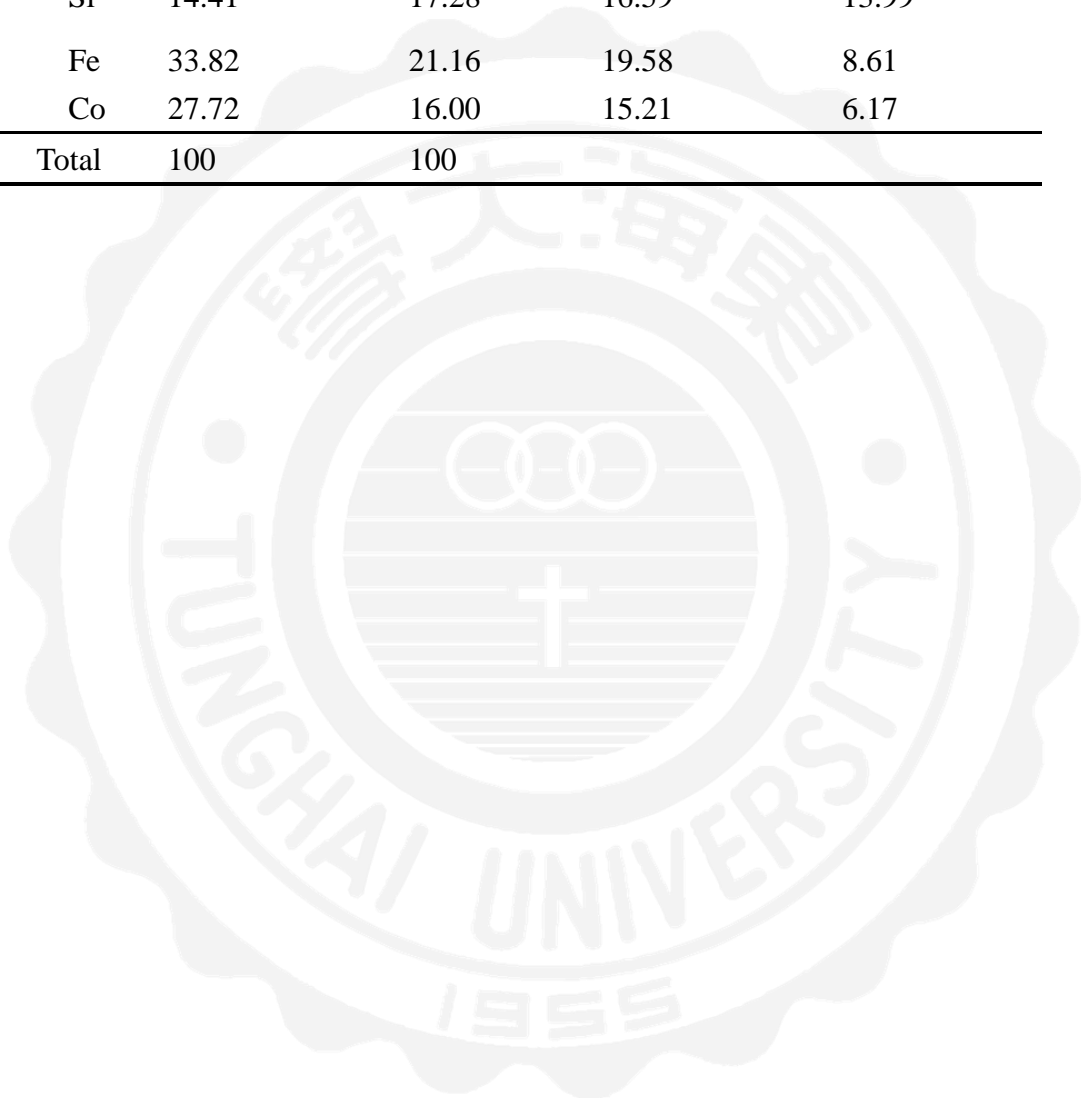


Figure 4.2. The SEM/EDS image of $\text{Fe}_3\text{O}_4/\text{SiO}_2/\text{Co}_3\text{O}_4$, (a) preparation with urea and (b) without urea.

Table 4.1 Analysis of elements on Fe₃O₄/SiO₂/Co₃O₄, (a) preparation with urea and (b) urea-free.

Element	Weight %		Atomic %	
	(a)	(b)	(a)	(b)
C		13.82		26.14
O	24.05	31.75	48.62	45.09
Si	14.41	17.28	16.59	13.99
Fe	33.82	21.16	19.58	8.61
Co	27.72	16.00	15.21	6.17
Total	100	100		



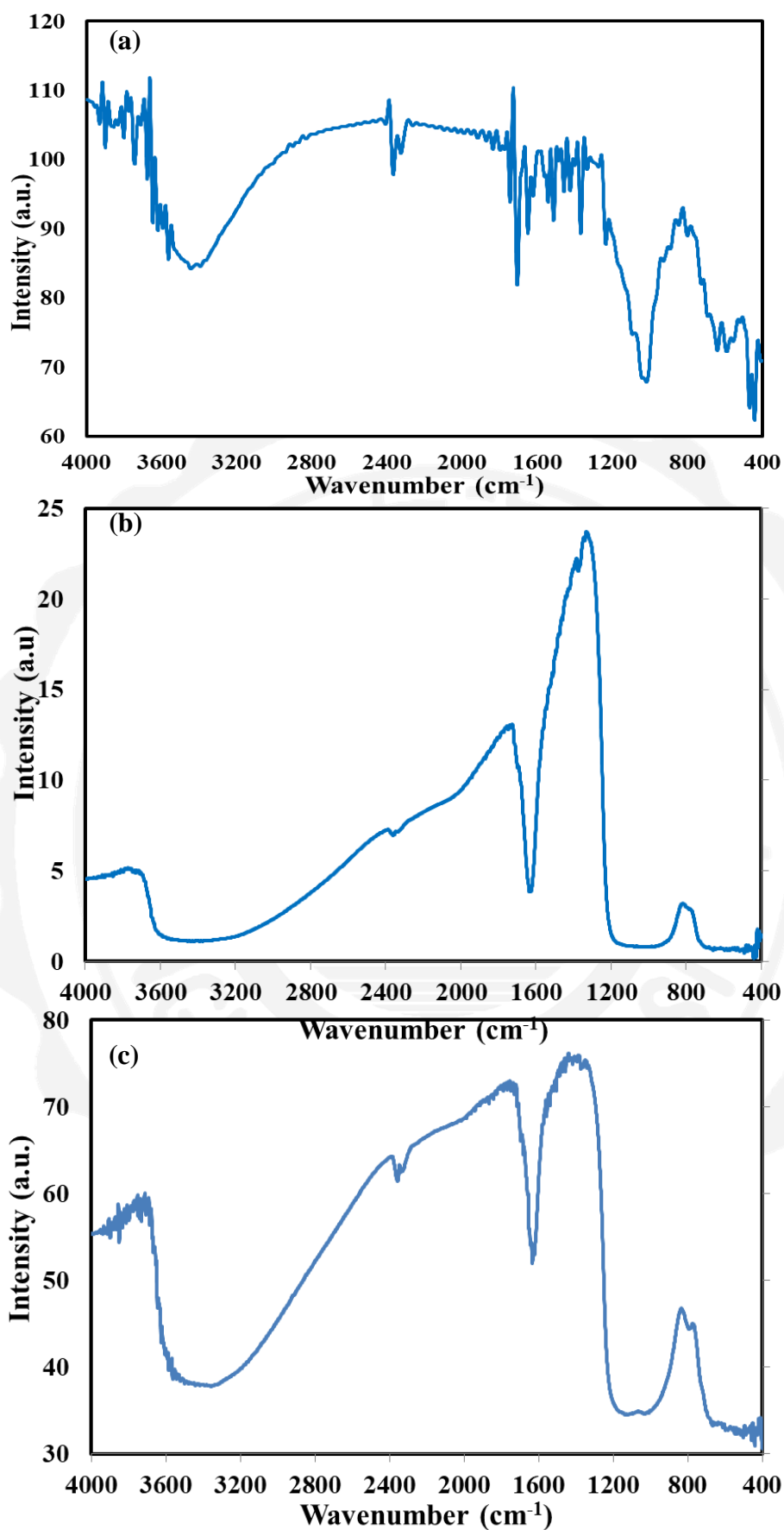
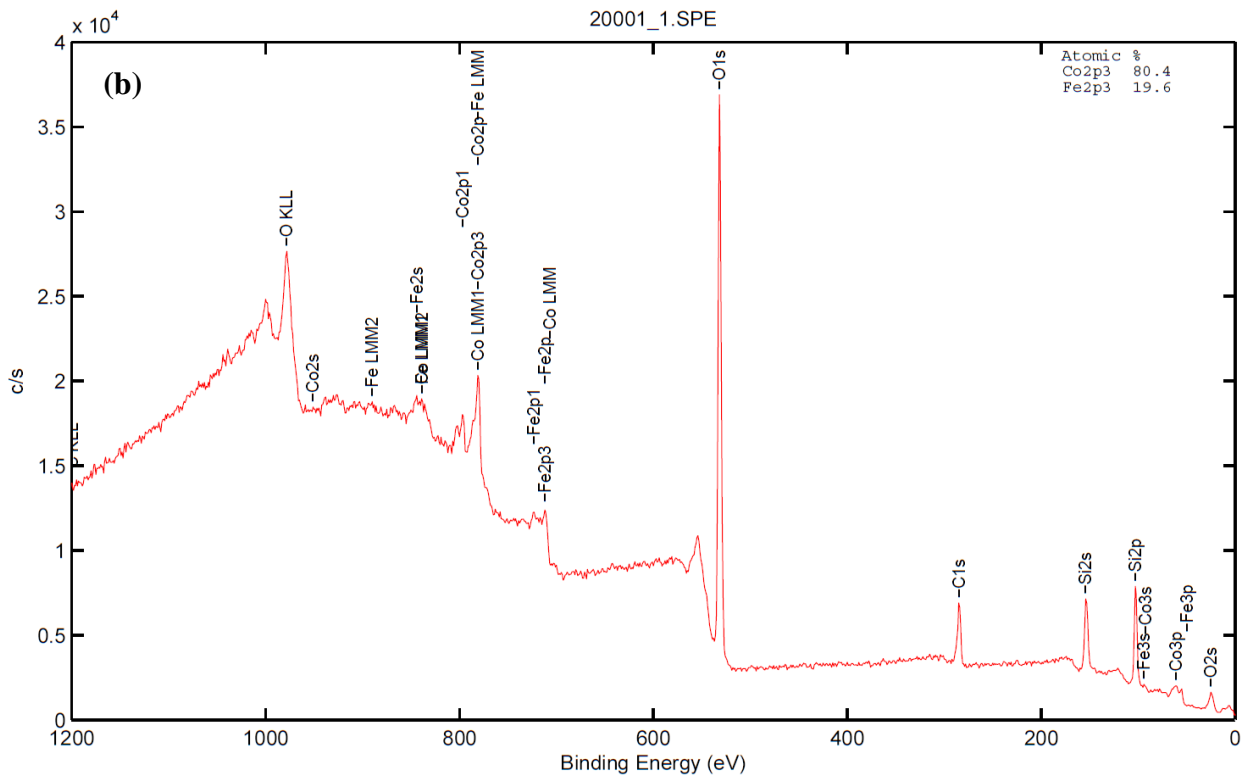
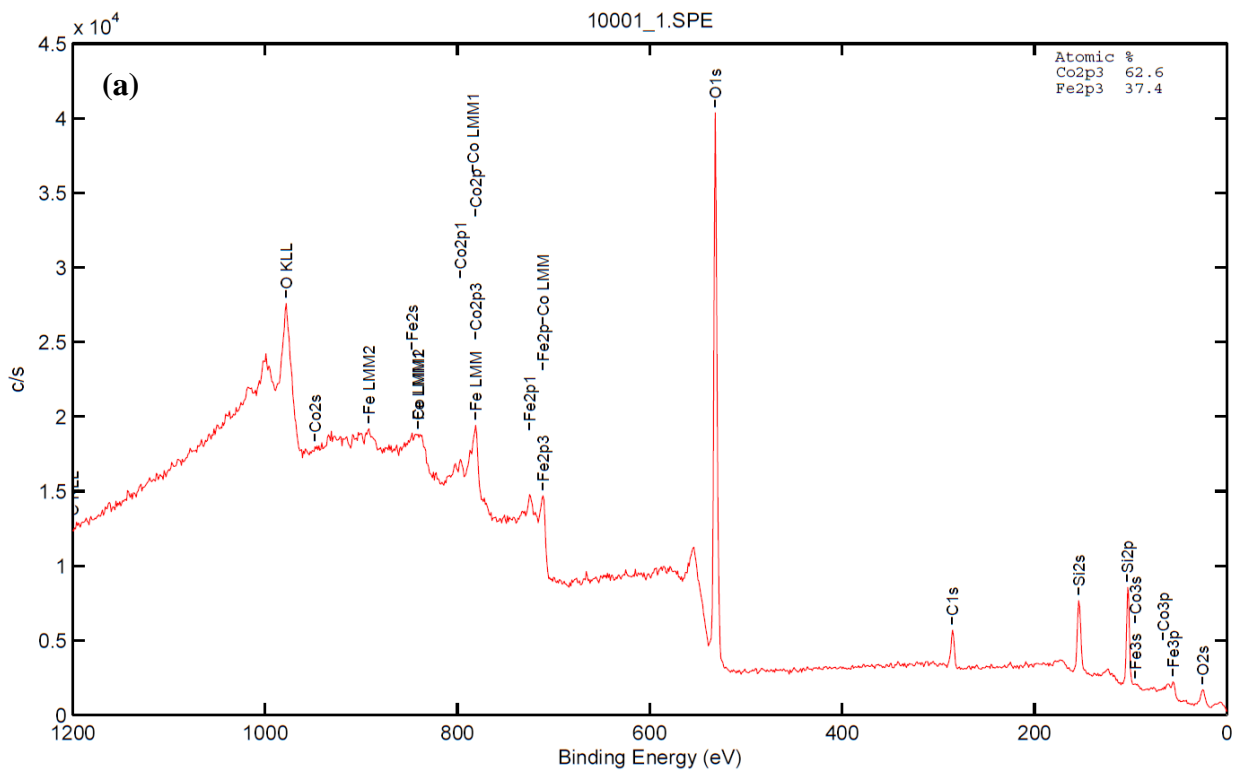


Figure 4.3. FTIR spectra of particles for preparation (a)with urea, (b) without urea and (c) with urea after calcined.



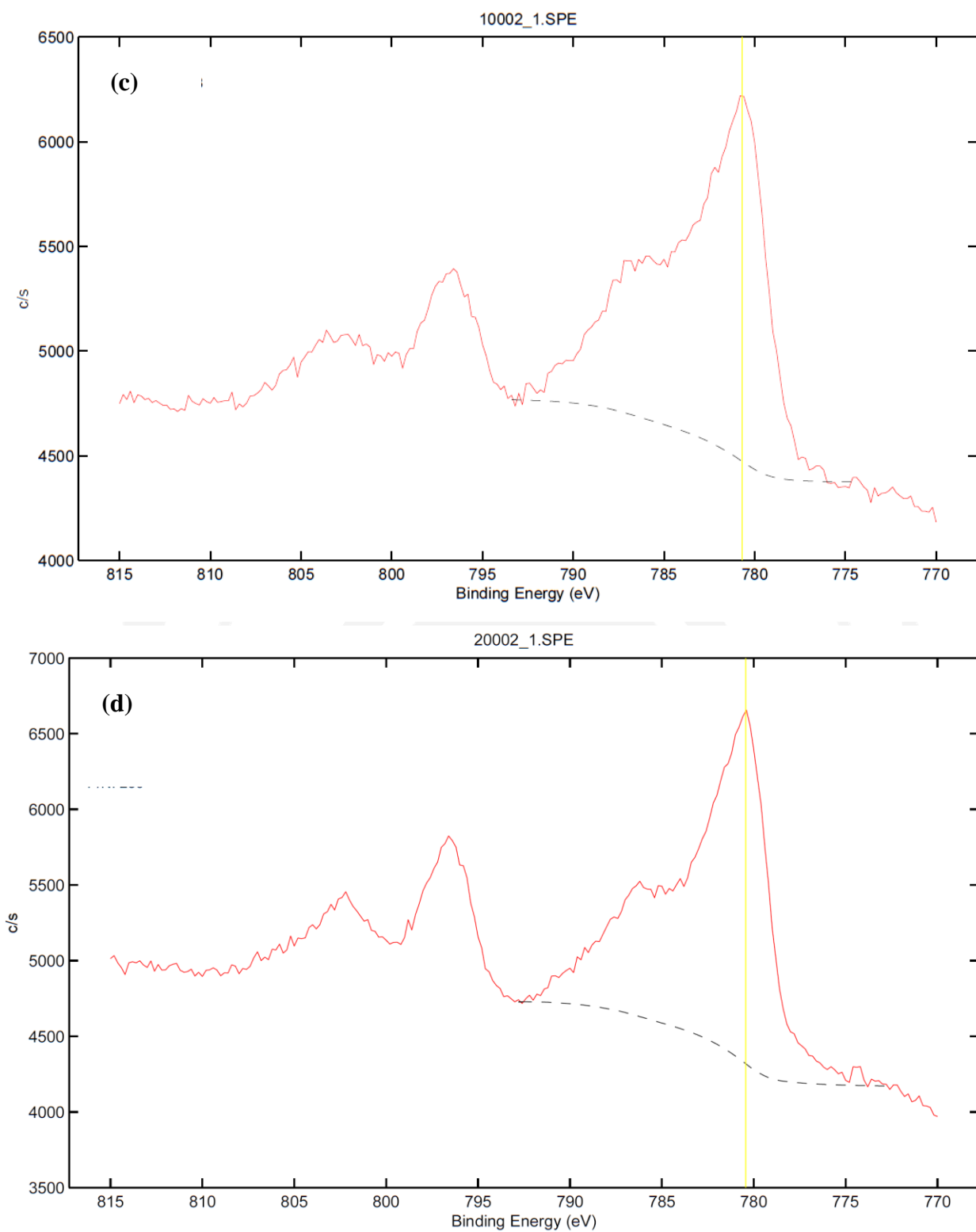


Figure 4.4 XPS spectrum of $\text{Fe}_3\text{O}_4/\text{SiO}_2/\text{Co}_3\text{O}_4$ and cobalt oxides, (a) urea-free and (b) urea-added are survey spectrum, (c) urea-free and (d) urea-added are Co2p.

Figure 4.3 showed the FTIR spectra of catalyst in different preparation of catalysts with or without urea, respectively. Characteristic peaks 1550-1457 cm^{-1} , attributed to stretching of N-O, are observed in urea-added group in figure 4.3 (a). After calcined, the surface particles have not appeared N-O bond anymore. The intensity of -OH were observed for both catalysts, 3438 cm^{-1} corresponding to stretching modes of O-H, implying that it might be an important reason for the catalyst's activity [27]. Vibration peaks of Co-O- in Co_3O_4 were observed at 664 cm^{-1} and 565 cm^{-1} [59], and the Co^{2+} and Co^{3+} ions gave two transmittance bands at around 565 cm^{-1} and 664 cm^{-1} , confirming the presence of Co_3O_4 . This result confirmed that the $\text{Co}(\text{NO}_3)_2$ as precursor in air led to the formation of Co_3O_4 at 673K calcined temperature.

XPS was further carried to investigate the metallic state of active species (Co) on $\text{Fe}_3\text{O}_4/\text{SiO}_2$. In XPS spectrum (Shown in figure 4.4), there are four peaks regarding to different cobalt species on $\text{Fe}_3\text{O}_4/\text{SiO}_2/\text{Co}_3\text{O}_4$. Peaks centered at 781.1 eV and 796.5 eV are characteristic of the Co_3O_4 [60]. The corresponding shake-up satellite peaks for these peaks are centered at 781.1 eV. The peak at 796.5 eV was a chemical shift of the main spin-orbit component, as a result that cobalt cation on the nanocrystal surface interacts with surface -OH, which were consistent with Xu's et al., 2016 results. Furthermore, cobalt-loading could be enhanced by adding urea. The atomic % of Co2P3 was 80.4% which is higher than that of urea-free group, 62.6%.

As shown in Figure 4.5, Fe_3O_4 , $\text{Fe}_3\text{O}_4/\text{SiO}_2$ and $\text{Fe}_3\text{O}_4/\text{SiO}_2/\text{Co}_3\text{O}_4$ catalyst exhibits superparamagnetism with magnetizations of 76.7, 27.1,

and 6.02 emu/g, respectively, at room temperature (25 °C). The catalyst could simply be separated by an external magnetic from the treated water.

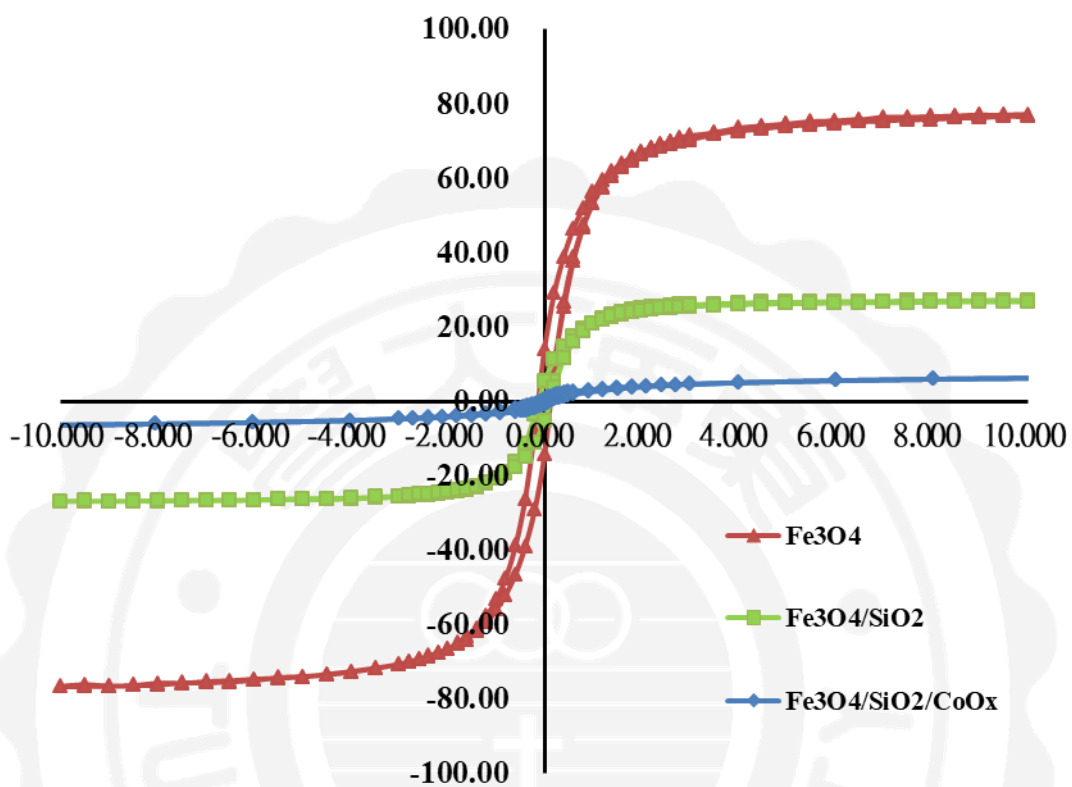


Figure 4.5 Analyses of field-dependent magnetization hysteresis for Fe₃O₄, Fe₃O₄/SiO₂ and Fe₃O₄/SiO₂/Co₃O₄.

The charge state of a catalyst surface depends on both the water pH and pH_{pzc} . Figure 4.6 illustrates the zeta potential of the $\text{Fe}_3\text{O}_4/\text{SiO}_2/\text{Co}_3\text{O}_4$ and $\text{Fe}_3\text{O}_4/\text{SiO}_2/\text{Mn-Pd}$ at various pH values, indicating that the pH_{pzc} were 4.73 and 11.9, respectively. Most of the surface hydroxyl groups were at the neutral state when the water pH was close to the pH_{pzc} .

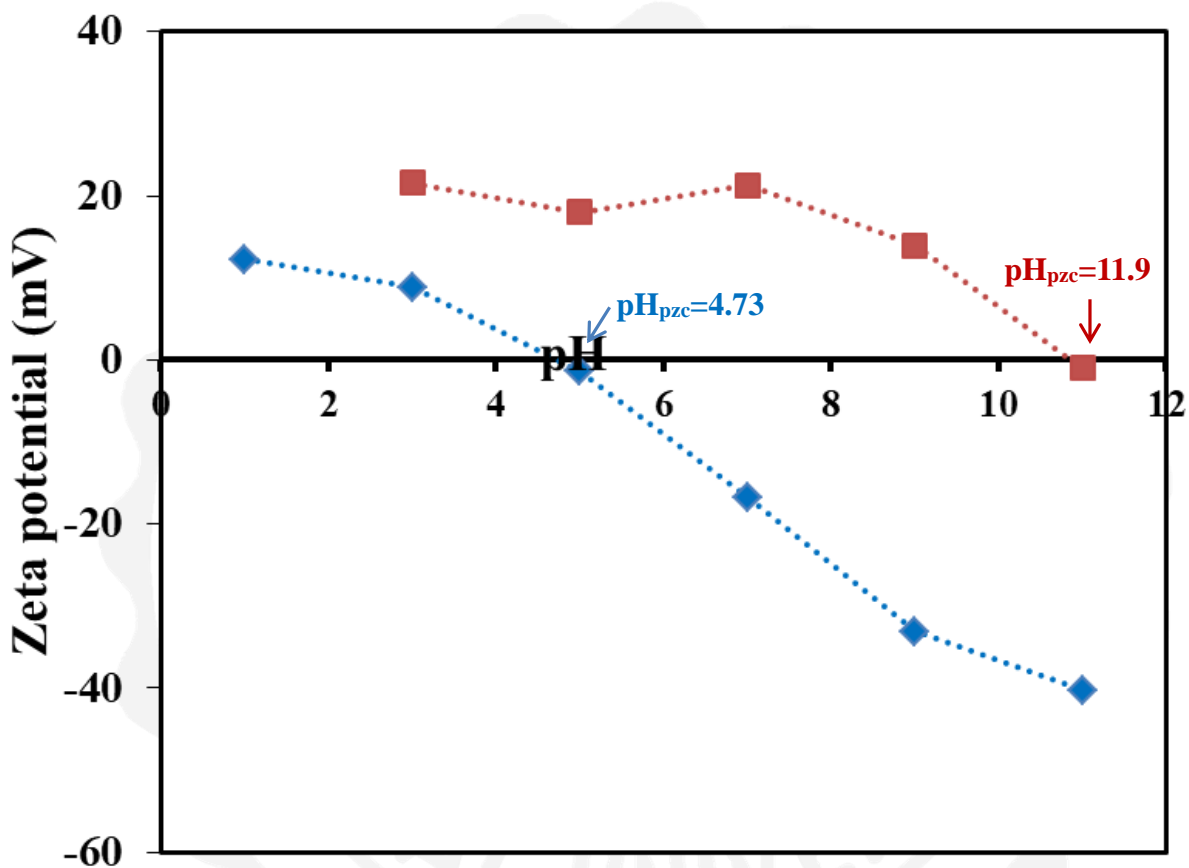


Figure 4.6 Zeta potential analysis of $\text{Fe}_3\text{O}_4/\text{SiO}_2/\text{Co}_3\text{O}_4$ and $\text{Fe}_3\text{O}_4/\text{SiO}_2/\text{Mn-Pd}$

4.1.1 Comparison of the characteristic between Fe₃O₄/SiO₂/Co₃O₄ and Fe₃O₄/SiO₂/Mn-Pd

EDS was illustrated that Pd and Mn were coated on the Fe₃O₄/SiO₂ at % of 2.40 and 1.66 and Co was coated at % of 27.72, which was shown in Table 4.2. The ratio may affect area of contact with ozone and potential of free radicals generated. The data may affect the subsequent results of decomposition at different pH of solution. The SQUID of Fe₃O₄/SiO₂/Co₃O₄ and Fe₃O₄/SiO₂/Mn-Pd were 6.02 and 22.5 emu/g [61], respectively. Fe₃O₄/SiO₂/Mn-Pd could be easier to recover the catalysts after experiments. The pH_{pzc} of Fe₃O₄/SiO₂/Co₃O₄ and Fe₃O₄/SiO₂/Mn-Pd were 4.73 and 10.9 and the results may affect reaction route. Hydroxyl radicals were produced due to the reaction between ozone and the surface of catalysts as a result of pH solution and pH_{pzc} [62].

Table 4.2 EDS and SQUID of Fe₃O₄/SiO₂/Co₃O₄ and Fe₃O₄/SiO₂/Mn-Pd [61].

	Fe ₃ O ₄ /SiO ₂ /Co ₃ O ₄	Fe ₃ O ₄ /SiO ₂ /Mn-Pd
Element (Weight %)		
O	24.05	43.28
Si	14.41	22.16
Fe	33.82	28.61
Co	27.72	
Mn		2.40
Pd		1.66
Total	100	100
SQUID		
Fe ₃ O ₄	76.7	42.7
Fe ₃ O ₄ /SiO ₂	27.1	23.6
Fe ₃ O ₄ /SiO ₂ /Cat.	6.02	22.5
pH_{pzc}	4.73	10.9

4.2 Comparison of decomposition of coumarin between

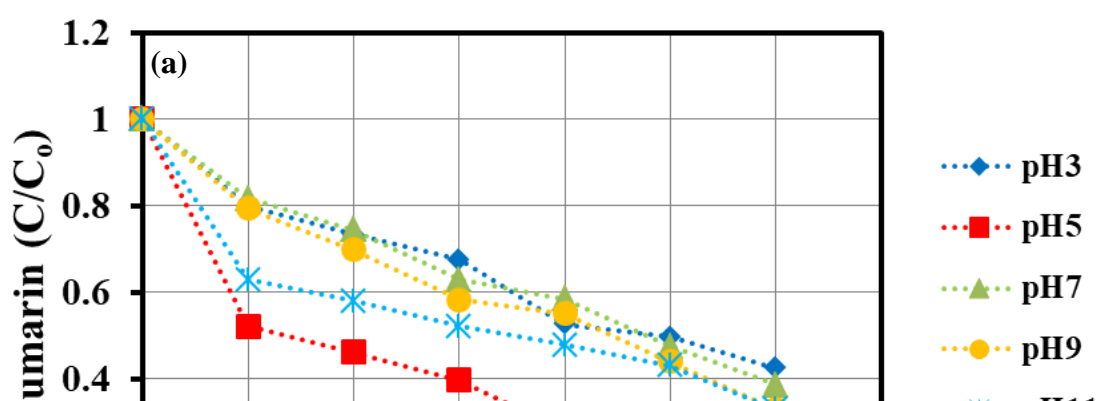
O₃/Fe₃O₄/SiO₂/Co₃O₄ and O₃/Fe₃O₄/SiO₂/Mn-Pd

pH is an important factor to investigate the mechanisms of catalytic ozonation, since it affects ozone decomposition. Furthermore, the properties of the surface catalysts and target pollutants being oxidized could be determined. The initial pH values (3, 5, 7, 9 and 11) of aqueous solutions were adjusted by hydrochloric acid and sodium hydroxide. Figure 4.7 shows the catalytic ozonation of decomposition of coumarin and the reaction constants are 2.9, 5.6, 2.7, 3.8 and 3.5 x 10⁻² min⁻¹ on O₃/Fe₃O₄/SiO₂/Co₃O₄ and 1.4, 1.3, 2.1, 4.6, and 6.0 x 10⁻² min⁻¹ on O₃/Fe₃O₄/SiO₂/Mn-Pd at pH 3, 5, 7, 9 and 11, respectively. The presence of Co₃O₄ catalyst during ozonation at pH 5 as well as Mn-Pd catalyst at pH 11 results in the production of hydroxyl radicals, which acts as strong oxidants. Catalyst which is covered by surface hydroxyl groups will be protonated or deprotonated when pH of solution is below or above pH_{pzc} [9]. Several studies have proved that the deprotonated or neutral surface hydroxyl groups had a strong reactivity toward ozone [63-65]. Negatively charged surface had a strong reactivity toward ozone and then the k_d values at pH 7 and 9 were higher than that of pH 3 which was protonated phenomena. The presence of a Pd–Mn catalyst during ozonation at pH 11 (pH_{pzc}=10.9) results in the production of hydroxyl radicals, which act as strong oxidants.

Coumarin is known to form the fluorescent compound, 7-hydroxycoumarin, in which it reacts with hydroxyl radicals in an aqueous solution. Co₃O₄ as catalysts had high activity to produce more hydroxyl radicals at pH 5 shown in figure 3.8. The reaction resulted in the formation of substantial amounts of 7-hydroxycoumarin after 25 minutes. The results

suggested that the degradation of coumarin was more efficient at pH 5 than at other pH values.

The comparison of the efficiency of catalysts between Co_3O_4 and Pd-Mn was shown in Table 4.3. The removal of coumarin was 78.3% and 84.7% for $\text{O}_3/\text{Fe}_3\text{O}_4/\text{SiO}_2/\text{Co}_3\text{O}_4$ and $\text{O}_3/\text{Fe}_3\text{O}_4/\text{SiO}_2/\text{Mn-Pd}$ in exceptional condition. The reaction constants (k_d) were 5.65×10^{-2} and 6.03×10^{-2} for $\text{O}_3/\text{Fe}_3\text{O}_4/\text{SiO}_2/\text{Co}_3\text{O}_4$ and $\text{O}_3/\text{Fe}_3\text{O}_4/\text{SiO}_2/\text{Mn-Pd}$, respectively. Although $\text{O}_3/\text{Fe}_3\text{O}_4/\text{SiO}_2/\text{Mn-Pd}$ had the highest constant value, removal rate and constants at low pH (3 and 5) were not expectable. The k_d values of $\text{O}_3/\text{Fe}_3\text{O}_4/\text{SiO}_2/\text{Co}_3\text{O}_4$ at high pH (7, 9 and 11) are above 3 min^{-1} . The formation of 7-hydroxycoumarin in $\text{O}_3/\text{Fe}_3\text{O}_4/\text{SiO}_2/\text{Co}_3\text{O}_4$ process was the highest (0.77 mg/L) at pH 5 and maintained above 0.60 mg/L at high pH (pH 9 and 11). The formation of 7-hydroxycoumarin in $\text{O}_3/\text{Fe}_3\text{O}_4/\text{SiO}_2/\text{Mn-Pd}$ process increased from 0.25 mg/L at pH 3 to 0.63 mg/L at pH 11. This increase can be attributed to the effect pH_{pzc} which was close to the pH of solution. According to the result shown in figure 3.9, it is clear to see that the set of experiment showed high effectiveness in the pH range.



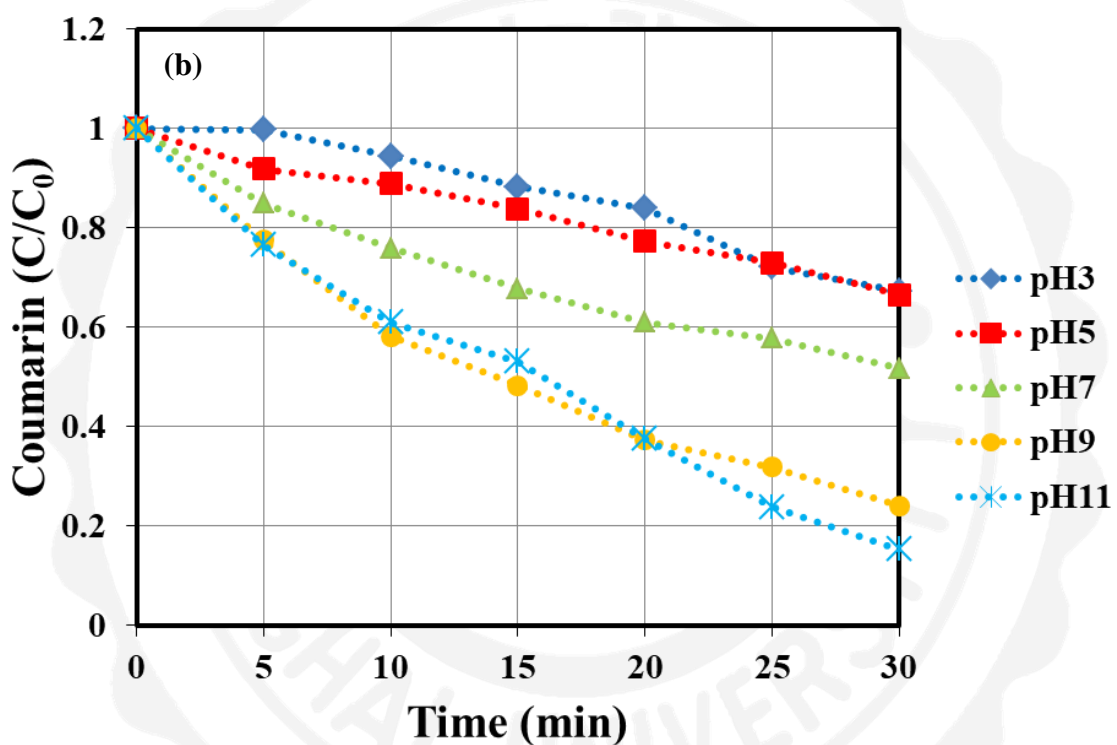
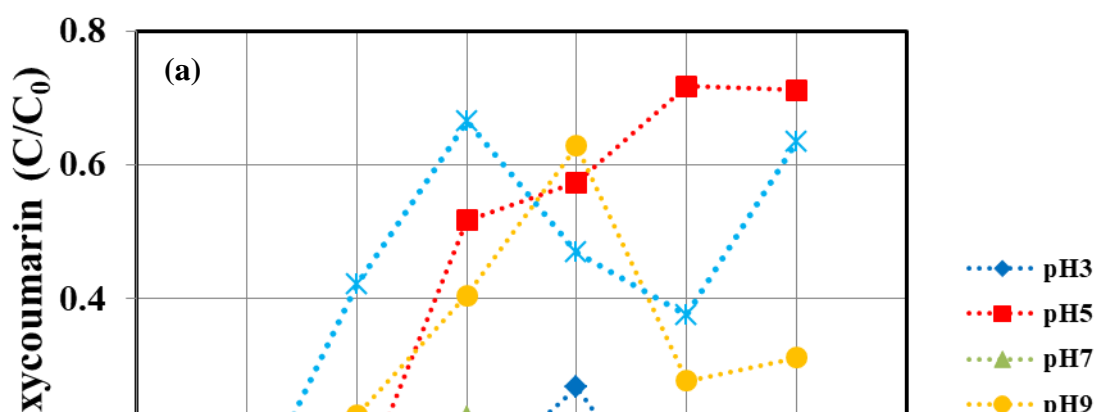


Figure 4.7 Effect of pH on coumarin removal by C/C_0 , (a) $O_3/Fe_3O_4/SiO_2/Co_3O_4$ and (b) $O_3/Fe_3O_4/SiO_2/Mn-Pd$ ($C_0=100$ mg/L, O_3 concentration = 1.6mg/L and catalyst dosage: 1.0g/L).



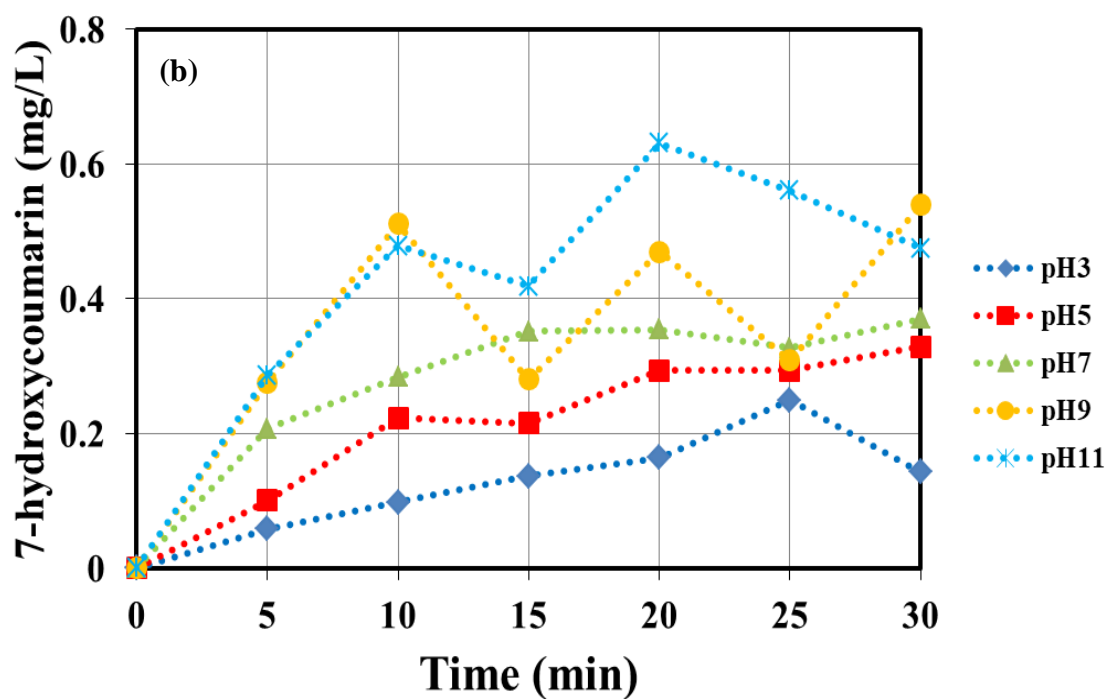


Figure 4.8 Effect of pH on the production of 7-hydroxycoumarin on (a) $O_3/Fe_3O_4/SiO_2/Co_3O_4$ and (b) $O_3/Fe_3O_4/SiO_2/Mn-Pd$ ($C_0=100$ mg/L, O_3 concentration = 1.6mg/L and catalyst dosage: 1.0g/L).

Table 4.3 The comparison between Mn-Pd and Co₃O₄ catalyst on catalytic ozonation of coumarin

Coumarin		O ₃ /Fe ₃ O ₄ /SiO ₂ /Co ₃ O ₄		O ₃ /Fe ₃ O ₄ /SiO ₂ /Mn-Pd	
		Removal rate%	k _d x10 ⁻² (min ⁻¹)	Removal rate%	k _d x10 ⁻² (min ⁻¹)
pH	3	57.7	2.92	32.7	1.40
	5	78.3	5.65	33.5	1.30
	7	61.5	3.03	48.3	2.12
	9	67.2	3.46	75.9	4.46
	11	67.3	3.82	84.7	6.03
7-hydroxycoumarin					
		Conc. (mgL ⁻¹)	Time (min)	Conc. (mgL ⁻¹)	Time (min)
pH	3	0.26	20	0.25	25
	5	0.71	25	0.33	30
	7	0.22	15	0.37	30
	9	0.63	20	0.54	30
	11	0.66	15	0.63	20

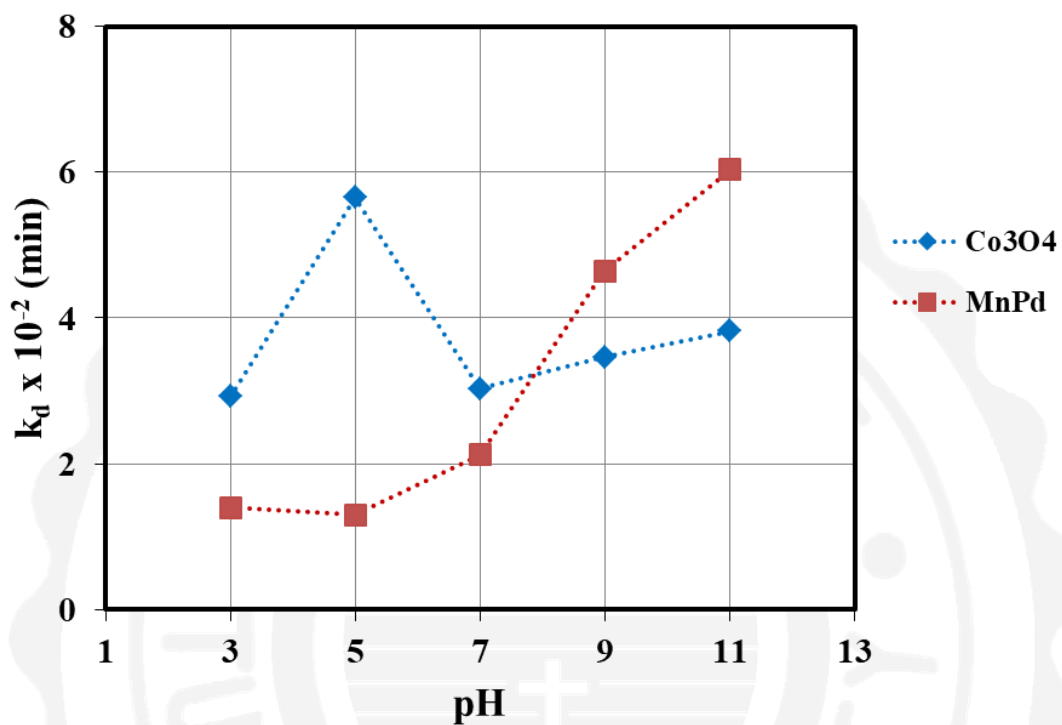


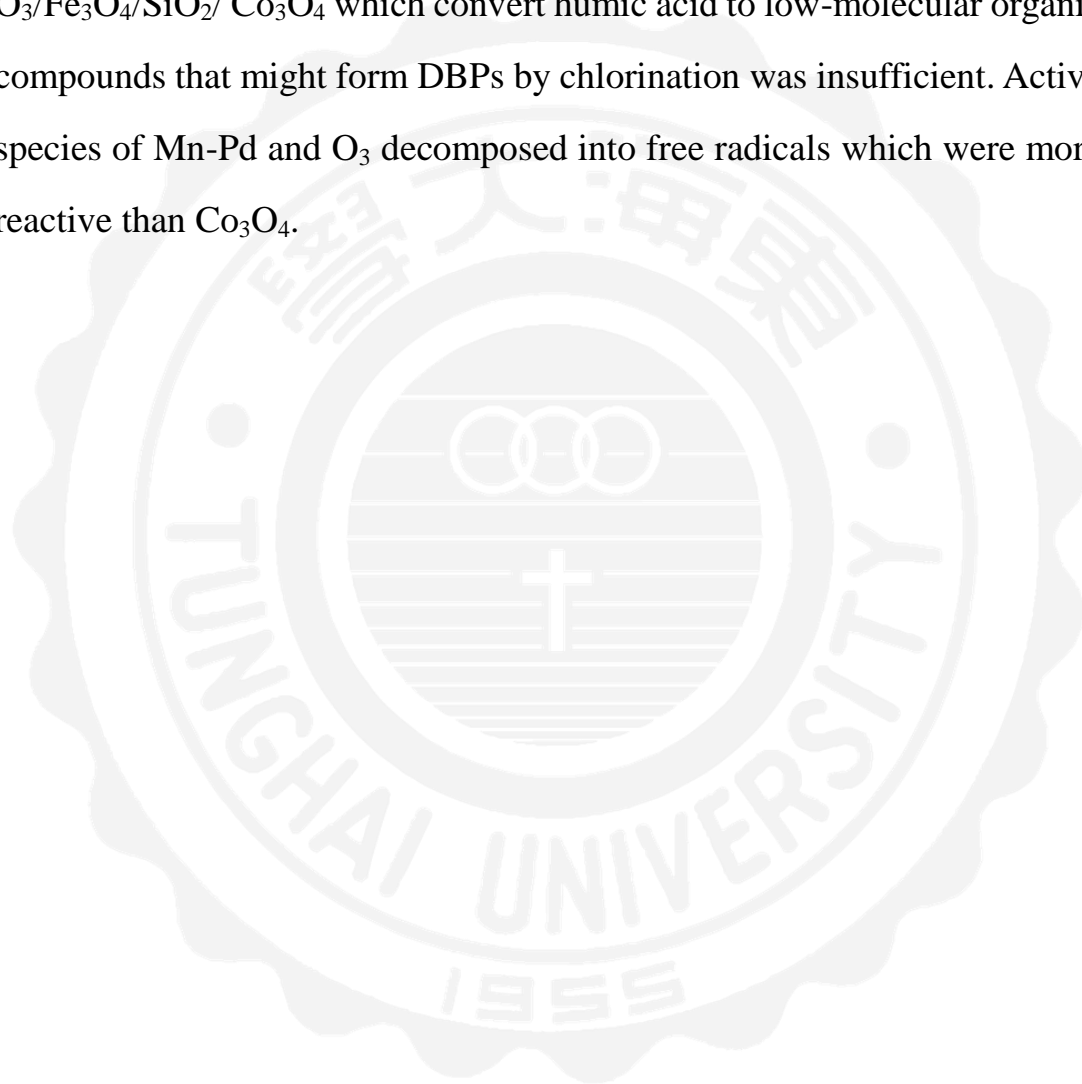
Figure 4.9 Effect of k_d value of coumarin at various pH on $O_3/Fe_3O_4/SiO_2/Co_3O_4$ and $O_3/Fe_3O_4/SiO_2/Mn-Pd$ (Experimental conditions: O_3 concentration = 1.6 mg/L, pH of $Fe_3O_4/SiO_2/Co_3O_4$ and $O_3/Fe_3O_4/SiO_2/Mn-Pd$ at 5 and 11, respectively).

4.3 Reduction of THMFPS by $O_3/Fe_3O_4/SiO_2/Co_3O_4$ and $O_3/Fe_3O_4/SiO_2/Mn-Pd$

Humic acid (HA) is a significant component of natural organic matter and has high molecular weight compounds [66]. It is difficult to determine the contents of HA because of the structural complexity, heterogeneous composition and variable chemical content [67]. The UV absorbance are surrogate parameters for the determination of HA concentration. The A_{254} represents the aromatic structure of organics in water. Figure 4.10 shows that UV absorbance changes of aqueous humic acid solution and DOC removal in a stream of ozone with the reaction time. Both of $O_3/Fe_3O_4/SiO_2/Co_3O_4$ and $O_3/Fe_3O_4/SiO_2/Mn-Pd$ had efficient decomposition of A_{254} and rates were 77.2% and 79.5%. A five-minute application of catalytic ozonation provided rapid degradation. The color changes of samples became lighter along the time, suggested that aromatic molecules of HA was destroyed from brown to light yellow. Turkey et al., 2014 proposed that it was 9% for sole ozonation. $O_3/Fe_3O_4/SiO_2/Mn-Pd$ at pH 11 was more effective than $O_3/Fe_3O_4/SiO_2/Co_3O_4$ process. DOC removal rates were 75.8% and 88.7% on $O_3/Fe_3O_4/SiO_2/Co_3O_4$ and $O_3/Fe_3O_4/SiO_2/Mn-Pd$ process, respectively. The results is similar to decomposition of coumarin and 7-hydroxycoumarin generated (See in Table 4.3) that $O_3/Fe_3O_4/SiO_2/Mn-Pd$ could produce more $\bullet OH$ and destroy refractory organic compounds such as humic acid more powerfully.

Chlorination is a common disinfection process used in most countries to treat drinking water. Figure 4.11 shows that the decomposition of NOM through catalytic ozonation followed by chlorination treatment to

investigate the formation of disinfection by-products. The inhibition rates of THMFPs on $O_3/Fe_3O_4/SiO_2/Mn-Pd$ and $O_3/Fe_3O_4/SiO_2/Co_3O_4$ process were 74.3% and 53.6%, respectively. It is obvious that $O_3/Fe_3O_4/SiO_2/Mn-Pd$ was more efficient to inhibit the THMFPs than that of $O_3/Fe_3O_4/SiO_2/Co_3O_4$ process. It suggested that the mineralization of $O_3/Fe_3O_4/SiO_2/Co_3O_4$ which convert humic acid to low-molecular organic compounds that might form DBPs by chlorination was insufficient. Active species of Mn-Pd and O_3 decomposed into free radicals which were more reactive than Co_3O_4 .



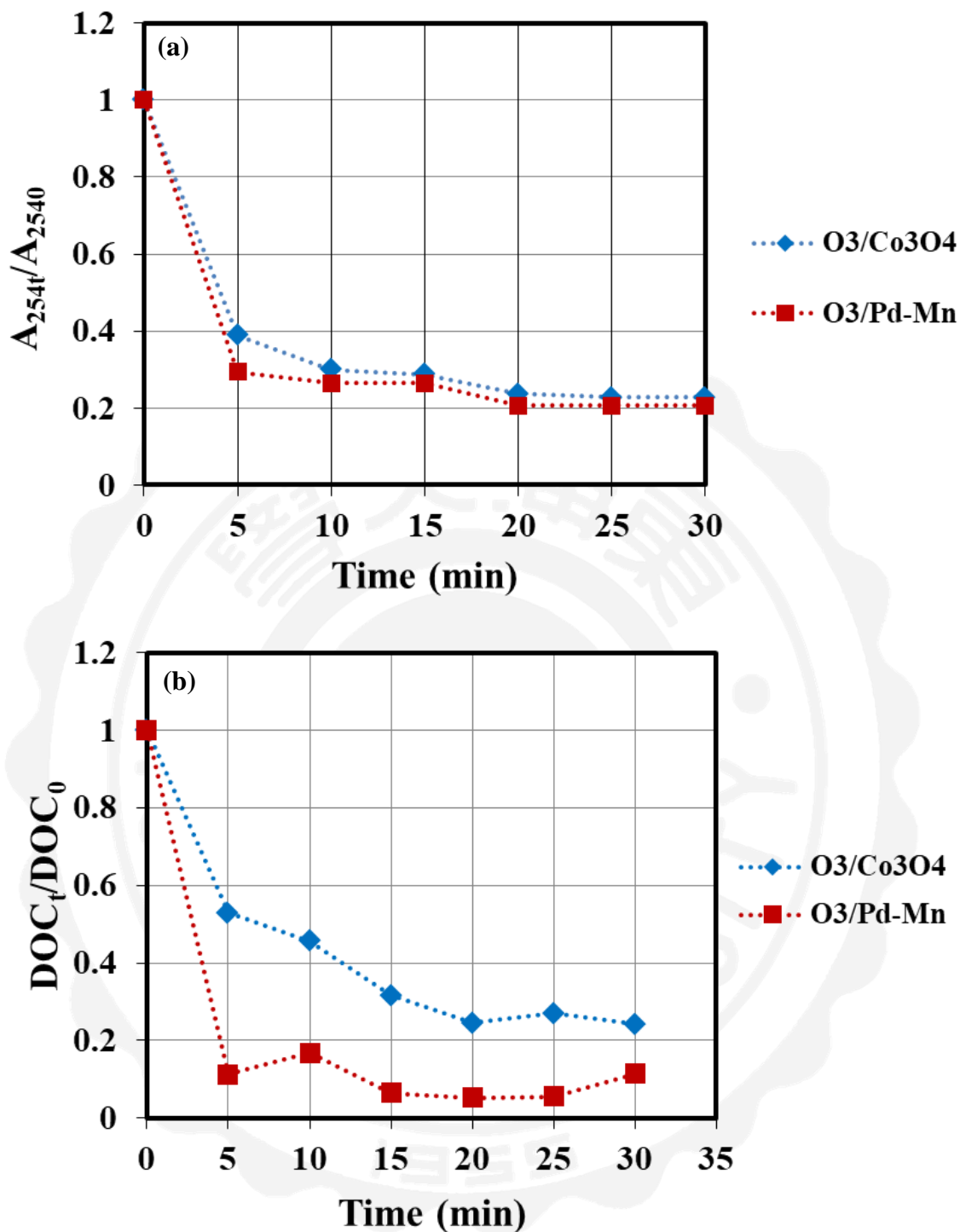


Figure 4.10 The effect of (a) A_{254} of NOMs decomposition and (b) DOC removal rates on O₃/Fe₃O₄/SiO₂/Co₃O₄ and O₃/Fe₃O₄/SiO₂/Mn-Pd (Experimental conditions: O₃ concentration = 1.6 mg/L, pH of Fe₃O₄/SiO₂/Co₃O₄ and O₃/Fe₃O₄/SiO₂/Mn-Pd at 5 and 11, respectively).

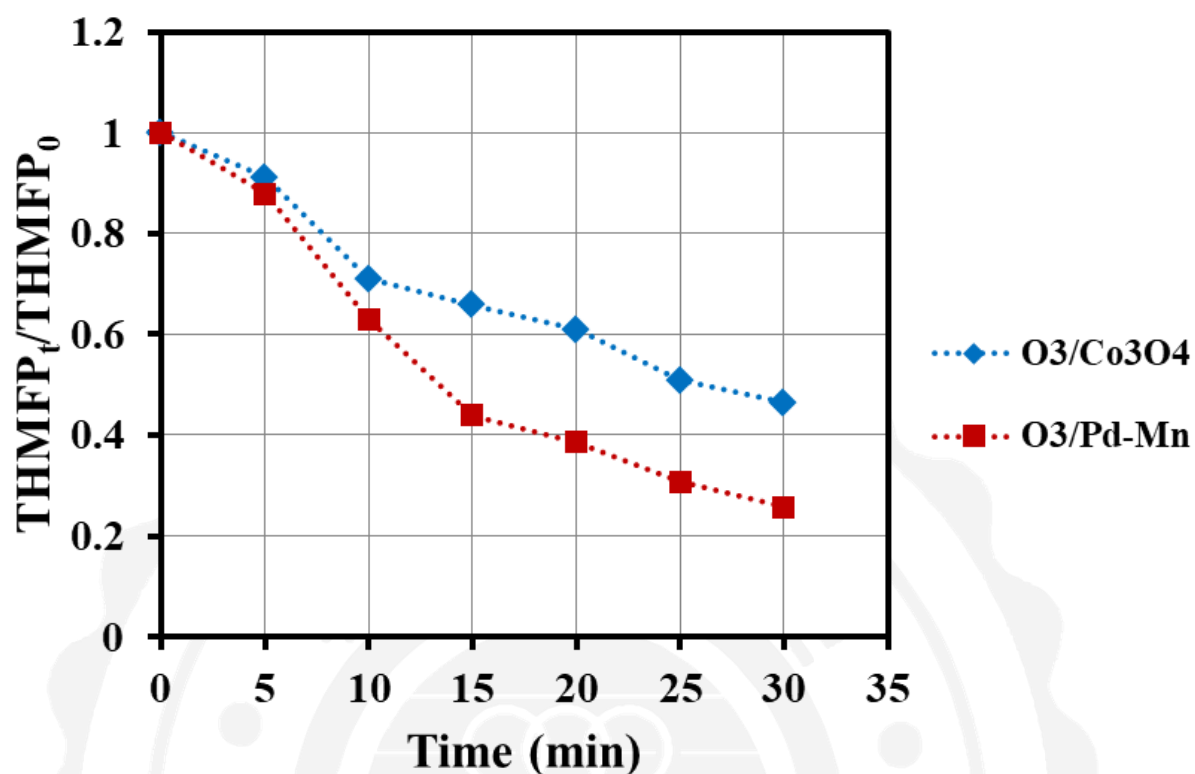


Figure 4.11 Comparison of THMFPs decompositions in O₃/Fe₃O₄/SiO₂/Co₃O₄ and O₃/Fe₃O₄/SiO₂/Mn-Pd (Experimental conditions: O₃ concentration = 1.6 mg/L, pH of Fe₃O₄/SiO₂/Co₃O₄ and O₃/Fe₃O₄/SiO₂/Mn-Pd at 5 and 11, respectively).

4.4 Catalytic ozonation of Methylene Blue by O₃/Fe₃O₄/SiO₂/Co₃O₄

According to the cost evaluation, Co₃O₄ would be used as a catalysts for catalytic ozonation of Methylene blue and diclofenac and investigate the efficient conditions and mechanism. Generally, heterogeneous catalytic ozonation mainly depends on the decomposition of ozone to be hydroxyl radicals of the reactant on catalyst surface. The pseudo first order reaction is used to represent the ozonation and catalytic ozonation by the following equation:

$$\frac{dC_A}{dt} = -k_R C_A \quad \text{eq. 9}$$

where k_R (min⁻¹) is the kinetic constant of the pseudo-heterogeneous catalytic ozonation (Li *et al.*, 2015). The logarithmic plot of the concentration of Methylene blue is shown in figure 4.11. The efficiency of removal methylene blue in catalytic ozonation in any conditions of pH is higher than that of SOP.

The rate constants are 0.118, 0.140, 0.137, 0.126, 0.125 and 0.123 min⁻¹ in condition of pH 3, 5, 7, 9 and 11, respectively (shown in figure 4.12). The results are consistence with the theory that pH of solution get more closed to pH_{pzc} can reach the activity of catalysts to generate more hydroxyl radicals to remove Methylene blue effectively. When the pH of solution is higher than pH_{pzc} , the catalysts become negative charged and might influence the adsorption of ozone on catalyst surface.

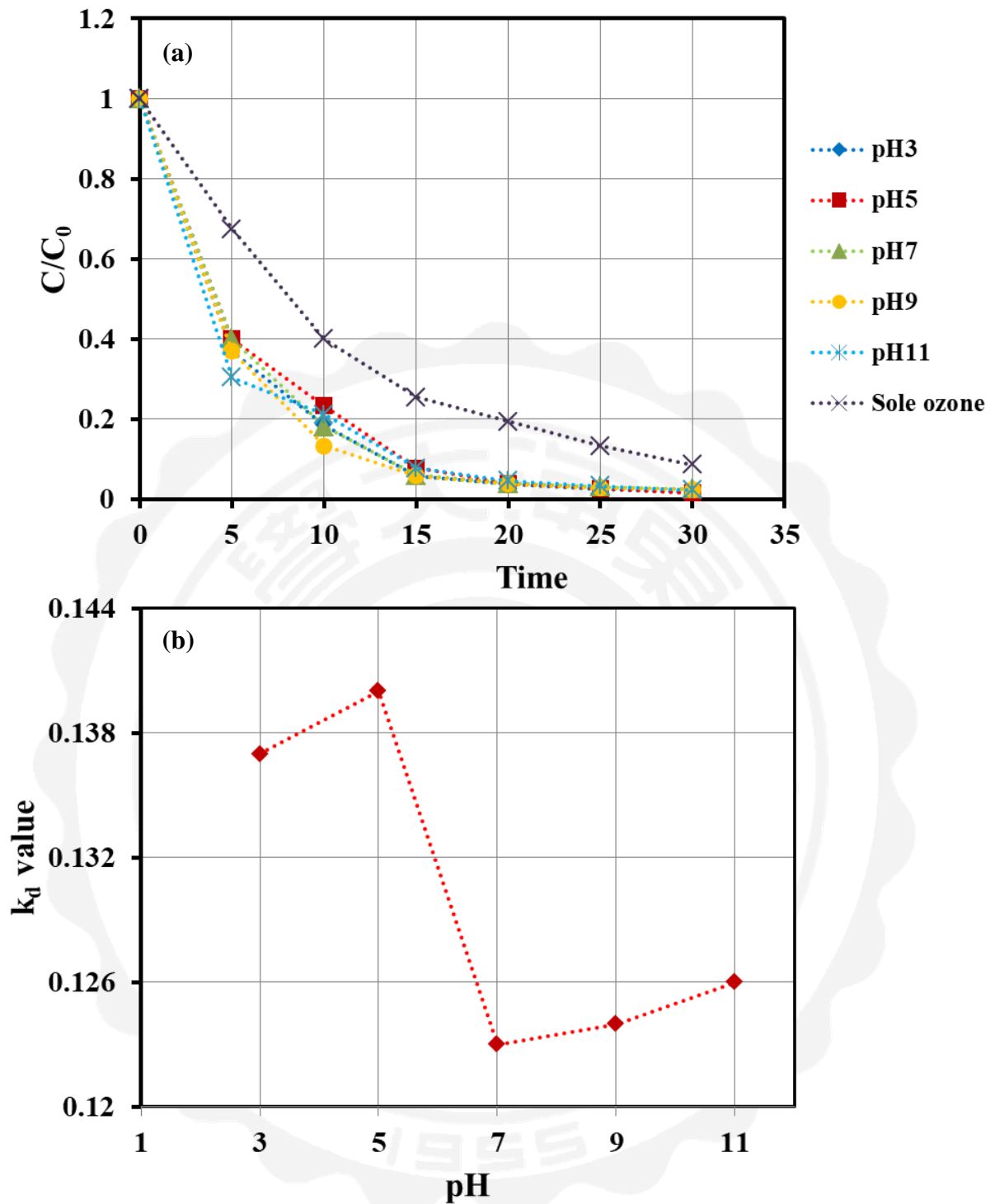


Figure 4.12 Effect of initial pH on degradation of Methylene Blue by catalytic ozonation (a) at various pH and (b) k_d value ($C_o=100$ mg/L, $O_3=1.6$ mg/L, initial dosage=1 g/L).

4.5 Decomposition of Diclofenac by $O_3/Fe_3O_4/SiO_2/Co_3O_4$

4.5.1 Dosage loading

In aqueous solution, the degradation of DCF by SOP and COP follows second-order kinetics (Eq.) [27], which can be simplified to pseudo first-order reaction kinetics when the oxidants and catalyst are over loaded. The usage of catalysts in aqueous solution is an important factor due to catalysts can provide active sites for catalytic reaction among water, ozone and organic compounds. In general, the reactive sites and surface areas increased with increase of catalyst dosage, and then decomposition of pollutants would be increased efficiently. In figure 4.13 showed the dosage effect on TOC removal of DCF and K_d value.

After 60 min reaction time, TOC removal was 46% in the presence of 0.5 g/L catalyst. As the catalyst dosage increasing to 1.0, 1.5 and 2.0 g/L, the TOC removal was 76%,80% and 86%, respectively. Dosage of from 1.0 increased to 2.0 g/L, the TOC removal had not to increase apparently.

The reaction rate constant (k_{obs}) for catalytic ozonation would obtain values of dosage 0, 0.5, 1.0, 1.5 and 2.0 g/L were 0.009, 0.0113, 0.0275, 0.0332 and 0.0331 min^{-1} , respectively, which was shown in figure 3.13 (b). Excessive amount of catalyst is insignificant efficiency. Therefore, it was necessary to optimize the catalyst dosage based on the experimental results.

However, with an excessive increase in the amount of active constituent, the catalyst showed a negative effect the DCF degradation, because (1) more active constituent might quench Reactive Oxygen

Species and (2) more active constituent loading might change the structure and surface properties of the catalyst, which would decrease the catalytic activity [27].



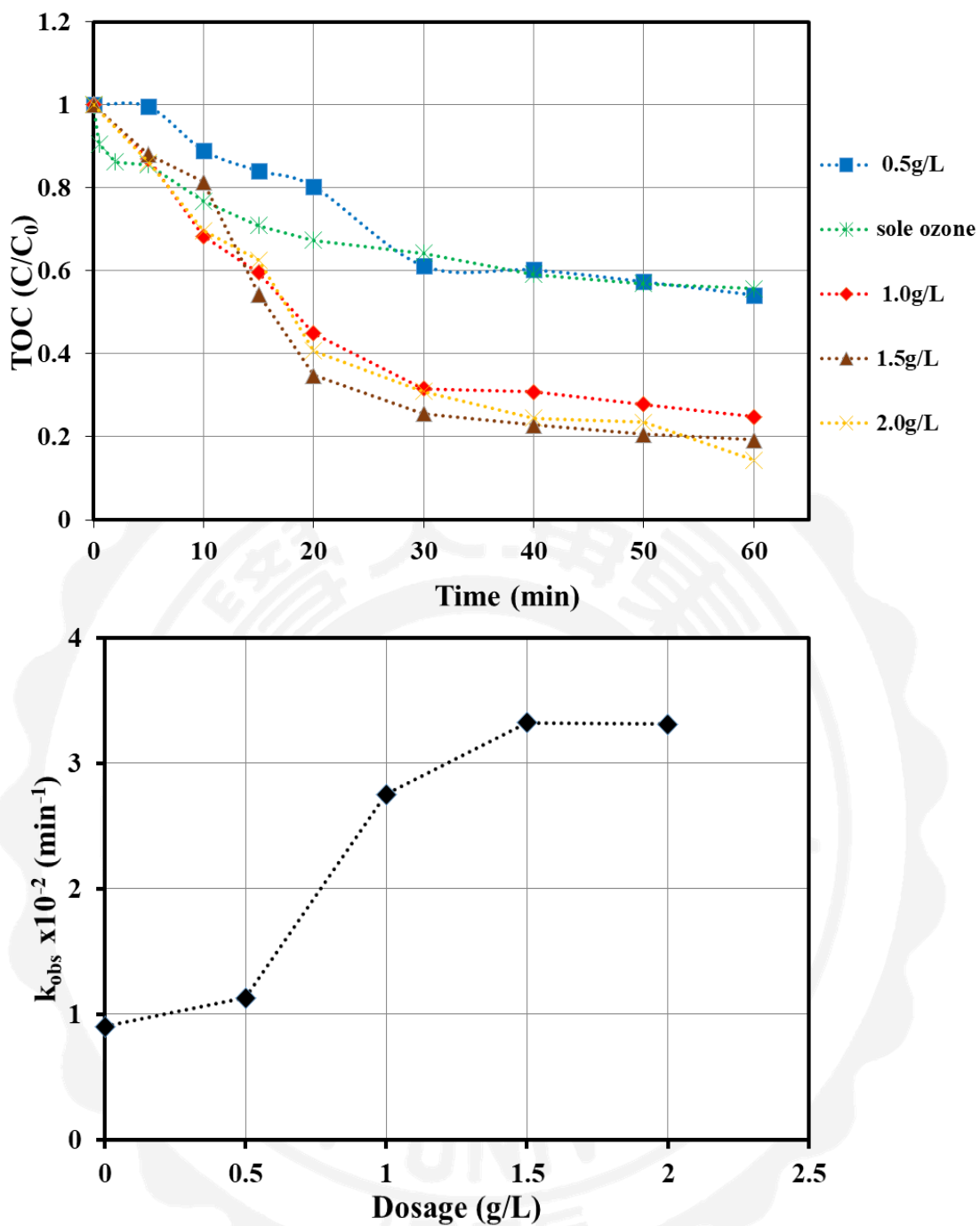


Figure 4.13 TOC removal (a) and k_{obs} value (b) at different doses of catalyst dosages (0.5, 1.0, 1.5, 2.0 g/L), (conditions of experiments: initial solution of DCF:50 mg/L; initial pH: 5, O₃=1.6 mg/L).

3.5.2 Effect of pH

The pH value of solution has great influence on both ozonation and catalytic ozonation due to its effect on the decomposition of ozone and surface properties of catalysts. In heterogeneous catalytic ozonation, the surface charge properties of catalyst which was involved in ozone decomposition and $\bullet\text{OH}$ generation directly are also influenced by pH of solution. Catalysts which were covered by surface hydroxyl groups will be protonated or deprotonated when pH of solution is below or above pH_{pzc} . As shown in figure 4.14, a better mineralization rate was achieved at neutral condition between catalyst and solution. The pH_{pzc} of catalyst was 4.73. Therefore, its surface hydroxyl groups will be generated and revealed in solution to be $\bullet\text{OH}$ which is more powerful oxidant. The surface hydroxyl groups were in deprotonated status when $\text{pH} > \text{pH}_{\text{pzc}}$, negatively charged surface had a strong reactivity toward ozone and $\bullet\text{OH}$ and then the rate of $\text{pH} > \text{pH}_{\text{pzc}}$ groups were higher than $\text{pH} < \text{pH}_{\text{pzc}}$ groups (at pH 3 condition). However, the TOC removal in catalytic ozonation is similar at different pH reached 68% to 76%.

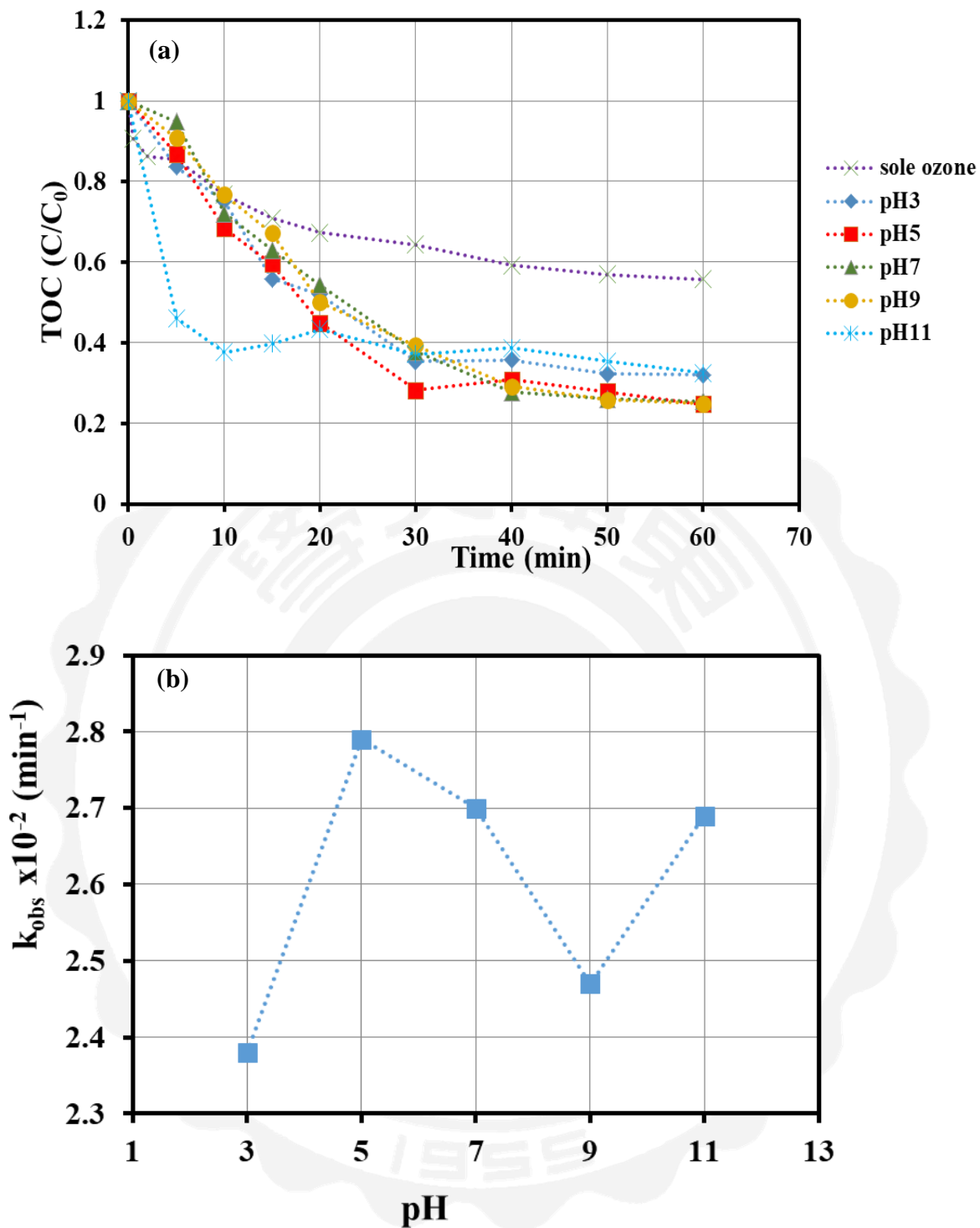


Figure 4.14 Effect of initial pH on (a)TOC removal and (b) k_{obs} value (conditions of experiments: initial solution of DCF:50 mg/L; catalyst concentration 1 g/L, $O_3=1.6$ mg/L).

3.5.3 Formation of Hydrogen peroxide

Hydrogen peroxide (H_2O_2) was important active species in catalytic ozonation process. It could be generated either from direct ozonation of unsaturated organics or the self-combined of $\bullet\text{OH}$ [9]. Qi et al., 2015 [23] proposed that H_2O_2 is a byproduct of the reaction between $\text{O}_3/\bullet\text{OH}$ and olefinic products resulting from the breaking of the aromatic moiety of the initial pollutants [23]. The $[\text{H}_2\text{O}_2]$ was increased to 4.13 mg/L and 3.91 mg/L evidently after 30 minute in COP of pH5 and pH11, respectively, since TOC degradation of DCF was ineffective after 30 minutes. The enhanced generation of H_2O_2 in catalytic ozonation has evidence for the development of DCF degradation shown in figure 4.15. The TOC was insignificant decreased after 30 minutes in COP of pH5 and pH11. In SOP of pH5, the maximum yield of H_2O_2 that was generated 2.28 mg/L at 60 minutes and it was the lowest of all reaction.

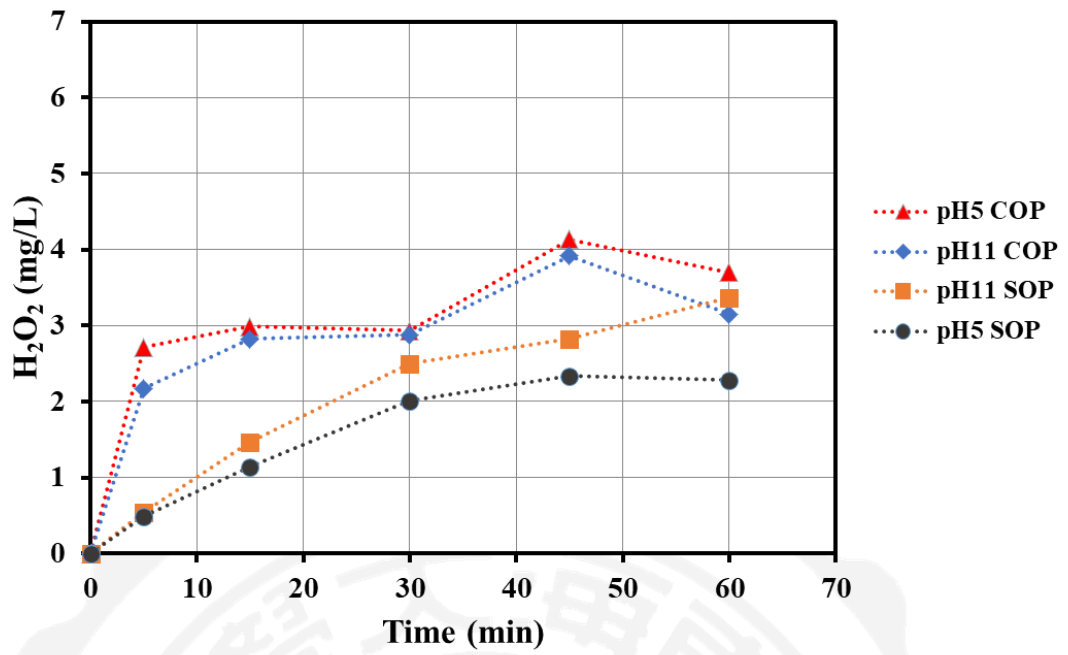


Figure 4.15 Generation of H_2O_2 in SOP and COP (conditions: initial concentration of DCF solution: 50 mg/L; catalyst concentration: 1g/L).

Chapter 4 Conclusion

EDS analysis was used to investigate the chemical composition of the catalyst, which suggests that the $\text{Fe}_3\text{O}_4/\text{SiO}_2/\text{Co}_3\text{O}_4$ are composed of Fe, O, Si and Co and weight % is 31.75, 17.28%, 21.16% and 16.00% for preparation without urea and 33.82, 24.05%, 14.41% and 27.72% for preparation with urea, respectively. Urea-added during the preparation could enhance to 13% of the content of cobalt. The FTIR spectra of catalysts indicated in different preparation of catalysts with or without urea, respectively. Characteristic peaks 1550-1457 cm^{-1} , attributed to stretching of N-O, are observed in urea-added group. After calcined, the surface particles have not appeared N-O bond anymore. The intensity of -OH were observed for both catalysts, 3438 cm^{-1} corresponding to stretching modes of O-H, suggesting that may be an important reason for the catalyst's activity. Vibration peaks of Co-O- in Co_3O_4 were observed at 664 cm^{-1} and 565 cm^{-1} , and the Co^{2+} and Co^{3+} ions gave two transmittance bands at around 565 cm^{-1} and 664 cm^{-1} , confirming the presence of Co_3O_4 . This results confirmed that the $\text{Co}(\text{NO}_3)_2$ as precursor in air led to the formation of Co_3O_4 at 673K calcined temperature. The XRD patterns of the Co_3O_4 (Dong *et al.*, 2010), the CoO_x on the $\text{Fe}_3\text{O}_4/\text{SiO}_2$ is existed in Co_3O_4 . the peaks at $2\theta=31.3^\circ$, 36.9° , 44.8° , 59.4° , and 62.9° ($d=1.43$) correspond to the (220), (311), (400), (511) and (440) planes of the Co_3O_4 cubic structure, respectively. However, the peaks were similar to those belongs to Fe_3O_4 . XPS are able to not only confirm the existence of cobalt but also obtain the valence of cobalt. Peaks centered at 781.1 eV and 796.5 eV are characteristic of the Co_3O_4 . The corresponding shake-up satellite peaks for

these peaks are centered at 781.1 eV. The peak at 796.5 eV was a chemical shift of the main spin-orbit components, as a result that cobalt cation on the nanocrystal surface interacts with surface –OH. $\text{Fe}_3\text{O}_4/\text{SiO}_2/\text{Mn-Pd}$ process catalyzed ozonation was more effective than $\text{O}_3/\text{Fe}_3\text{O}_4/\text{SiO}_2/\text{Co}_3\text{O}_4$ process for DOC removals of coumarin, humic acid and the reductions of disinfection by-products formation potential in the treatment of natural water. The formation of 7-hydroxycoumarin on $\text{O}_3/\text{Fe}_3\text{O}_4/\text{SiO}_2/\text{Mn-Pd}$ process was more than that of $\text{O}_3/\text{Fe}_3\text{O}_4/\text{SiO}_2/\text{Co}_3\text{O}_4$, suggested that the amount of $\bullet\text{OH}$ in $\text{Fe}_3\text{O}_4/\text{SiO}_2/\text{Mn-Pd}$ process was more than $\text{O}_3/\text{Fe}_3\text{O}_4/\text{SiO}_2/\text{Co}_3\text{O}_4$ process. $\text{O}_3/\text{Fe}_3\text{O}_4/\text{SiO}_2/\text{Co}_3\text{O}_4$ of Methylene Blue and Diclofenac those had the optimal condition of pH at 5 due to pH of solution closed to pH_{pzc} can reach the activity of catalysts to generate more $\bullet\text{OH}$ revealed from the surface hydroxyl groups of catalysts. Dosage of from 1.0 increased to 2.0 g/L, the TOC removal had not to increase apparently. With an excessive increase in the amount of active constituent, the catalyst showed a negative effect the DCF degradation, because (1) more active constituent might quench Reactive Oxygen Species and (2) more active constituent loading might change the structure and surface properties of the catalyst, which would decrease the catalytic activity [27].

References

- [1] D.C. McDowell, M.M. Huber, M. Wagner, U. von Gunten, T.A. Ternes, Ozonation of carbamazepine in drinking water: identification and kinetic study of major oxidation products, *Environmental science & technology*, 39 (2005) 8014-8022.
- [2] F. Am Water Works Res, B. Langlais, D.A. Reckhow, D.R. Brink, *Ozone in water treatment: application and engineering*, CRC press, 1991.
- [3] F.J. Beltrán, *Ozone reaction kinetics for water and wastewater systems*, crc Press, 2003.
- [4] W.H. Glaze, Reaction products of ozone: a review, *Environmental Health Perspectives*, 69 (1986) 151.
- [5] J. Hoigné, H. Bader, Rate constants of reactions of ozone with organic and inorganic compounds in water—II: dissociating organic compounds, *Water research*, 17 (1983) 185-194.
- [6] J. Hoigné, H. Bader, Rate constants of reactions of ozone with organic and inorganic compounds in water—I: non-dissociating organic compounds, *Water Research*, 17 (1983) 173-183.
- [7] P. Faria, D. Monteiro, J. Órfão, M. Pereira, Cerium, manganese and cobalt oxides as catalysts for the ozonation of selected organic compounds, *Chemosphere*, 74 (2009) 818-824.
- [8] S. Tong, R. Shi, H. Zhang, C. Ma, Catalytic performance of Fe₃O₄-CoO/Al₂O₃ catalyst in ozonation of 2-(2, 4-dichlorophenoxy) propionic acid, nitrobenzene and oxalic acid in water, *Journal of Environmental Sciences*, 22 (2010) 1623-1628.
- [9] W. Chen, X. Li, Z. Pan, S. Ma, L. Li, Effective mineralization of Diclofenac by catalytic ozonation using Fe-MCM-41 catalyst, *Chemical Engineering Journal*, 304 (2016) 594-601.
- [10] A. Rey, E. Mena, A. Chávez, F. Beltrán, F. Medina, Influence of structural properties on the activity of WO₃ catalysts for visible light photocatalytic ozonation, *Chemical Engineering Science*, 126 (2015) 80-90.
- [11] S. Zhang, D. Wang, S. Zhang, X. Zhang, P. Fan, Ozonation and carbon-assisted ozonation of methylene blue as model compound: effect of solution pH, *Procedia Environmental Sciences*, 18 (2013) 493-502.
- [12] S. Song, Z. Liu, Z. He, A. Zhang, J. Chen, Y. Yang, X. Xu, Impacts of morphology and crystallite phases of titanium oxide on the catalytic ozonation of phenol, *Environmental science & technology*, 44 (2010) 3913-3918.
- [13] N. Chokshi, B. Mehta, J. Ruparelia, *Catalytic Ozonation: Promising and Effective Method for Dye Wastewater*.

- [14] L. Liotta, M. Gruttadauria, G. Di Carlo, G. Perrini, V. Librando, Heterogeneous catalytic degradation of phenolic substrates: catalysts activity, *Journal of Hazardous Materials*, 162 (2009) 588-606.
- [15] M. Skoumal, P.-L. Cabot, F. Centellas, C. Arias, R.M. Rodríguez, J.A. Garrido, E. Brillas, Mineralization of paracetamol by ozonation catalyzed with Fe 2+, Cu 2+ and UVA light, *Applied Catalysis B: Environmental*, 66 (2006) 228-240.
- [16] D.S. Pines, D.A. Reckhow, Effect of dissolved cobalt (II) on the ozonation of oxalic acid, *Environmental science & technology*, 36 (2002) 4046-4051.
- [17] C.-H. Wu, C.-Y. Kuo, C.-L. Chang, Homogeneous catalytic ozonation of CI Reactive Red 2 by metallic ions in a bubble column reactor, *Journal of hazardous materials*, 154 (2008) 748-755.
- [18] Z. Ma, L. Zhu, X. Lu, S. Xing, Y. Wu, Y. Gao, Catalytic ozonation of p-nitrophenol over mesoporous Mn–Co–Fe oxide, *Separation and Purification Technology*, 133 (2014) 357-364.
- [19] Y. Guo, L. Yang, X. Cheng, X. Wang, The application and reaction mechanism of catalytic ozonation in water treatment, *Journal of Environmental and Analytical Toxicology*, 2 (2012) 1-6.
- [20] S.A. Taghavi, M. Moghadam, I. Mohammadpoor-Baltork, S. Tangestaninejad, V. Mirkhani, A.R. Khosropour, V. Ahmadi, Investigation of the catalytic activity of an electron-deficient vanadium (IV) tetraphenylporphyrin: A new, highly efficient and reusable catalyst for ring-opening of epoxides, *Polyhedron*, 30 (2011) 2244-2252.
- [21] Y. Dong, G. Wang, P. Jiang, A. Zhang, L. Yue, X. Zhang, Catalytic ozonation of phenol in aqueous solution by Co 3 O 4 nanoparticles, *Bulletin of the Korean Chemical Society*, 31 (2010) 2830-2834.
- [22] B. Legube, N.K.V. Leitner, Catalytic ozonation: a promising advanced oxidation technology for water treatment, *Catalysis Today*, 53 (1999) 61-72.
- [23] F. Qi, B. Xu, W. Chu, Heterogeneous catalytic ozonation of phenacetin in water using magnetic spinel ferrite as catalyst: Comparison of surface property and efficiency, *Journal of Molecular Catalysis A: Chemical*, 396 (2015) 164-173.
- [24] Y. Huang, C. Cui, D. Zhang, L. Li, D. Pan, Heterogeneous catalytic ozonation of dibutyl phthalate in aqueous solution in the presence of iron-loaded activated carbon, *Chemosphere*, 119 (2015) 295-301.
- [25] M. Sui, S. Xing, L. Sheng, S. Huang, H. Guo, Heterogeneous catalytic ozonation of ciprofloxacin in water with carbon nanotube supported manganese oxides as catalyst, *Journal of hazardous materials*, 227 (2012) 227-236.
- [26] Q. Bao, K. San Hui, J.G. Duh, Promoting catalytic ozonation of phenol over graphene through nitrogenation and Co 3 O 4 compositing, *Journal of Environmental Sciences*, 50 (2016) 38-48.

- [27] B. Xu, F. Qi, J. Zhang, H. Li, D. Sun, D. Robert, Z. Chen, Cobalt modified red mud catalytic ozonation for the degradation of bezafibrate in water: catalyst surface properties characterization and reaction mechanism, *Chemical Engineering Journal*, 284 (2016) 942-952.
- [28] J. Nawrocki, B. Kasprzyk-Hordern, The efficiency and mechanisms of catalytic ozonation, *Applied Catalysis B: Environmental*, 99 (2010) 27-42.
- [29] A. Ikhtlaq, D.R. Brown, B. Kasprzyk-Hordern, Mechanisms of catalytic ozonation on alumina and zeolites in water: formation of hydroxyl radicals, *Applied Catalysis B: Environmental*, 123 (2012) 94-106.
- [30] H. Valdés, V.J. Farfán, J.A. Manoli, C.A. Zaror, Catalytic ozone aqueous decomposition promoted by natural zeolite and volcanic sand, *Journal of Hazardous Materials*, 165 (2009) 915-922.
- [31] F.J. Stevenson, Organic forms of soil nitrogen, American Society of Agronomy, Crop Science Society of America, Soil Science Society of America, 1982.
- [32] J.J. Molnar, J.R. Agbaba, B.D. Dalmacija, M.T. Klačnja, M.B. Dalmacija, M.M. Kragulj, A comparative study of the effects of ozonation and TiO₂-catalyzed ozonation on the selected chlorine disinfection by-product precursor content and structure, *Science of the Total Environment*, 425 (2012) 169-175.
- [33] M. Kitis, J.E. Kilduff, T. Karanfil, Isolation of dissolved organic matter (DOM) from surface waters using reverse osmosis and its impact on the reactivity of DOM to formation and speciation of disinfection by-products, *Water research*, 35 (2001) 2225-2234.
- [34] D. Gümüş, F. Akbal, A comparative study of ozonation, iron coated zeolite catalyzed ozonation and granular activated carbon catalyzed ozonation of humic acid, *Chemosphere*, 174 (2017) 218-231.
- [35] J. Oldenburg, E.M. Quenzel, U. Harbrecht, A. Fregin, W. Kress, C.R. Müller, H.J. Hertfelder, R. Schwaab, H.H. Brackmann, P. Hanfland, Missense mutations at ALA-10 in the factor IX propeptide: an insignificant variant in normal life but a decisive cause of bleeding during oral anticoagulant therapy, *British journal of haematology*, 98 (1997) 240-244.
- [36] M. Rafatullah, O. Sulaiman, R. Hashim, A. Ahmad, Adsorption of methylene blue on low-cost adsorbents: a review, *Journal of hazardous materials*, 177 (2010) 70-80.
- [37] C.E. Zubieta, P.V. Messina, C. Luengo, M. Dennehy, O. Pieroni, P.C. Schulz, Reactive dyes removal by porous TiO₂-chitosan materials, *Journal of Hazardous materials*, 152 (2008) 765-777.
- [38] J. Wu, M.A. Eiteman, S.E. Law, Evaluation of membrane filtration and ozonation processes for treatment of reactive-dye wastewater, *Journal of environmental engineering*, 124 (1998) 272-277.

- [39] B. Owens, Pharmaceuticals in the environment: a growing problem, accessed CSR in the pharmaceutical industry, 203 (2015).
- [40] K.H.H. Aziz, H. Miessner, S. Mueller, D. Kalass, D. Moeller, I. Khorshid, M.A.M. Rashid, Degradation of pharmaceutical diclofenac and ibuprofen in aqueous solution, a direct comparison of ozonation, photocatalysis, and non-thermal plasma, *Chemical Engineering Journal*, (2016).
- [41] J. Schwaiger, H. Ferling, U. Mallow, H. Wintermayr, R. Negele, Toxic effects of the non-steroidal anti-inflammatory drug diclofenac: Part I: histopathological alterations and bioaccumulation in rainbow trout, *Aquatic Toxicology*, 68 (2004) 141-150.
- [42] F.J. Beltrán, P. Pocostales, P. Alvarez, A. Oropesa, Diclofenac removal from water with ozone and activated carbon, *Journal of Hazardous Materials*, 163 (2009) 768-776.
- [43] T. Huang, G. Zhang, S. Chong, Y. Liu, N. Zhang, S. Fang, J. Zhu, Effects and mechanism of diclofenac degradation in aqueous solution by US/ZnO, *Ultrasonics Sonochemistry*, 37 (2017) 676-685.
- [44] J. Gou, Q. Ma, Y. Cui, X. Deng, H. Zhang, X. Cheng, X. Li, M. Xie, Q. Cheng, H. Liu, Visible light photocatalytic removal performance and mechanism of diclofenac degradation by Ag₃PO₄ sub-microcrystals through response surface methodology, *Journal of Industrial and Engineering Chemistry*, (2017).
- [45] S. Chong, G. Zhang, Z. Wei, N. Zhang, T. Huang, Y. Liu, Sonocatalytic degradation of diclofenac with FeCeO_x particles in water, *Ultrasonics Sonochemistry*, 34 (2017) 418-425.
- [46] M.M. Huber, S. Canonica, G.-Y. Park, U. Von Gunten, Oxidation of pharmaceuticals during ozonation and advanced oxidation processes, *Environmental Science & Technology*, 37 (2003) 1016-1024.
- [47] A. Aguinaco, F.J. Beltrán, J.F. García-Araya, A. Oropesa, Photocatalytic ozonation to remove the pharmaceutical diclofenac from water: influence of variables, *Chemical engineering journal*, 189 (2012) 275-282.
- [48] A. Mashayekh-Salehi, G. Moussavi, K. Yaghmaeian, Preparation, characterization and catalytic activity of a novel mesoporous nanocrystalline MgO nanoparticle for ozonation of acetaminophen as an emerging water contaminant, *Chemical Engineering Journal*, 310 (2017) 157-169.
- [49] Y. Yang, J. Ma, Q. Qin, X. Zhai, Degradation of nitrobenzene by nano-TiO₂ catalyzed ozonation, *Journal of Molecular Catalysis A: Chemical*, 267 (2007) 41-48.
- [50] F. Nawaz, H. Cao, Y. Xie, J. Xiao, Y. Chen, Z.A. Ghazi, Selection of active phase of MnO₂ for catalytic ozonation of 4-nitrophenol, *Chemosphere*, 168 (2017) 1457-1466.
- [51] L. Yang, C. Hu, Y. Nie, J. Qu, Catalytic ozonation of selected pharmaceuticals over

mesoporous alumina-supported manganese oxide, *Environmental science & technology*, 43 (2009) 2525-2529.

[52] F.J. Beltrán, J.P. Pocostales, P.M. Alvarez, J. Jaramillo, Mechanism and kinetic considerations of TOC removal from the powdered activated carbon ozonation of diclofenac aqueous solutions, *Journal of hazardous materials*, 169 (2009) 532-538.

[53] L. Wang, A. Liu, Z. Zhang, B. Zhao, Y. Xia, Y. Tan, Catalytic ozonation of thymol in reverse osmosis concentrate with core/shell Fe₃O₄@ SiO₂@ Yb₂O₃ catalyst: Parameter optimization and degradation pathway, *Chinese Journal of Chemical Engineering*, (2016).

[54] G. Gao, J. Shen, W. Chu, Z. Chen, L. Yuan, Mechanism of enhanced diclofenac mineralization by catalytic ozonation over iron silicate-loaded pumice, *Separation and Purification Technology*, 173 (2017) 55-62.

[55] X. Cheng, Q. Cheng, X. Deng, P. Wang, H. Liu, A facile and novel strategy to synthesize reduced TiO₂ nanotubes photoelectrode for photoelectrocatalytic degradation of diclofenac, *Chemosphere*, 144 (2016) 888-894.

[56] S. Bao, L. Tang, K. Li, P. Ning, J. Peng, H. Guo, T. Zhu, Y. Liu, Highly selective removal of Zn (II) ion from hot-dip galvanizing pickling waste with amino-functionalized Fe₃O₄@ SiO₂ magnetic nano-adsorbent, *Journal of colloid and interface science*, 462 (2016) 235-242.

[57] A.P.H. Association, Water Environment Federation (APHA-AWWA-WEF). 2005, Standard Methods for the Examination of Water and Wastewater, 21st ed. Alexandria, Virginia: Water Environment Federation.

[58] H. reversible Co₃O₄, graphene hybrid anode for lithium rechargeable batteries Kim, Haegyeom; Seo, Dong-Hwa; Kim, Sung-Wook; Kim, Jongsoon; Kang, Kisuk, *Carbon*, 49 (2010) 326-332.

[59] G. Mekhemer, H. Abd-Allah, S. Mansour, Surface characterization of silica-supported cobalt oxide catalysts, *Colloids and Surfaces A: Physicochemical and Engineering Aspects*, 160 (1999) 251-259.

[60] R. Xu, H.C. Zeng, Mechanistic investigation on self-redox decompositions of Cobalt– Hydroxide– Nitrate compounds with different nitrate anion configurations in interlayer space, *Chemistry of materials*, 15 (2003) 2040-2048.

[61] L.-W. Lu, Y.-P. Peng, C.-N. Chang, Catalytic ozonation by palladium–manganese for the decomposition of natural organic matter, *Separation and Purification Technology*, (2017).

[62] S. Li, Y. Tang, W. Chen, Z. Hu, X. Li, L. Li, Heterogeneous catalytic ozonation of clofibric acid using Ce/MCM-48: preparation, reaction mechanism, comparison with Ce/MCM-41, *Journal of Colloid and Interface Science*, (2017).

[63] L. Zhao, J. Ma, Z. Sun, X. Zhai, Mechanism of influence of initial pH on the

degradation of nitrobenzene in aqueous solution by ceramic honeycomb catalytic ozonation, *Environmental science & technology*, 42 (2008) 4002-4007.

[64] S. Xing, C. Hu, J. Qu, H. He, M. Yang, Characterization and reactivity of MnO_x supported on mesoporous zirconia for herbicide 2, 4-D mineralization with ozone, *Environmental science & technology*, 42 (2007) 3363-3368.

[65] M. Ernst, F. Lurot, J.-C. Schrotter, Catalytic ozonation of refractory organic model compounds in aqueous solution by aluminum oxide, *Applied Catalysis B: Environmental*, 47 (2004) 15-25.

[66] B. Kasprzyk-Hordern, U. Raczyk-Stanisławiak, J. Świetlik, J. Nawrocki, Catalytic ozonation of natural organic matter on alumina, *Applied Catalysis B: Environmental*, 62 (2006) 345-358.

[67] O. Turkay, H. Inan, A. Dimoglo, Experimental and theoretical investigations of CuO-catalyzed ozonation of humic acid, *Separation and Purification Technology*, 134 (2014) 110-116.

